Obtaining backwater length estimates in modern and ancient fluvio-deltaic settings: review and proposal of standardized workflows

Van Yperen, A.E., Holbrook, J.M., Poyatos-Moré, M., Midtkandal, I.

@AnnaVanYperen

Obtaining backwater length estimates in modern and ancient fluvio-deltaic settings: review and proposal of standardized workflows

Van Yperen, A.E.[1], Holbrook, J.M.[2], Poyatos-Moré, M.[3], Midtkandal, I.[1]

[1]University of Oslo, Department of Geosciences, P.O. Box 1047 Blindern, 0316 Oslo, Norway

[2]Texas Christian University, Department of Geological Sciences, TCU Box 298830, Fort Worth, Texas 76129

[3]Universitat Autònoma de Barcelona, Department of Geology, Edifici C, 08193 Bellaterra (Cerdanyola del Vallès), Spain

Corresponding autor: a.v.yperen@geo.uio.no

Highlights

- Backwater length (Lb) predicts changes in channel morphology and sedimentary trends.
- Due to input parameter ambiguity, same river Lb estimates may vary a factor 6s
- In modern settings, Lb based on grain size and discharge are the least accurate
- In ancient settings, Lb based on grains size and bankfull channel depth is most reliable
- Proposed and tested workflows improve uncertainty management and comparability

Abstract

The backwater effect (i.e. channel flow influence by a body of standing water) is used to predict down-dip changes in fluvial morphodynamics and consequent sediment distribution on delta plains. These changes include downstream fining, decrease in sinuosity, and deepening and narrowing of channel belt deposits. This study reviews existing methods for estimating backwater length in ancient and modern settings and proposes workflows to minimize ambiguity in resultant estimates.

The proposed workflows are tailored to both modern and ancient settings and are prioritized based on practicality, accuracy, smallest uncertainty ranges and allow different types of data as input parameters. In modern river systems, we recommend using direct field measurements of bankfull thalweg channel depth and river water elevation to determine the location where riverbed elevation intersects sea level (i.e. the upstream limit of the backwater zone). Alternatively, the backwater length (Lb) can be estimated indirectly by Lb = h/S, with h is bankfull thalweg channel depth and S is slope. In ancient settings, bankfull thalweg depth and grain size representative of bedload transport are the most reliably measurable parameters, obtained at one or a few locations.

For the first time, the application of multiple methods to obtain backwater length estimates are tested on a single modern and ancient river system. In the modern case study, the riverbed intersection with sea level matches previously documented major changes in sedimentary trends, such as decreasing channel-belt width/thickness ratios, decreasing meander-bend migration rates, and coarsening grain size followed by distinct downstream fining. However, backwater lengths based on h/S plot downstream of this zone characterized by major changes, when input parameters are derived from discharge and grain size. Therefore, we recommend obtaining bankfull thalweg channel depth from a cross-sectional profile if backwater length is estimated based on h/S. In the ancient case study, bankfull thalweg channel depth derived from fully preserved single story channel fill and slope based on Shields' empirical relation with grain size, match changes in fluvial architectural style interpreted as a result of backwater effects. Although uncertainty management is improved with the proposed workflows, a

degree of uncertainty remains in the resulting backwater length estimates, due to inherent scatter in previously established relationships (e.g. Shields stress relation to obtain slope estimates).

This review is a critical step forward in discussing the shortcomings, and listing and acknowledging the uncertainties and ambiguity in obtaining the necessary input parameters to estimate backwater lengths. The proposed workflows facilitate comparability and applicability of future backwater length estimates and their corresponding influence on the hydrodynamic environment and ultimately the stratigraphic record. Potential scaling relationships between the backwater length, sedimentary trends and avulsion nodes makes this of key importance as the latter two also play a crucial role in devastating floods when rivers change course.

Keywords: backwater effect, backwater length, source to sink, fluvio-deltaic strata, modern river systems

1. Introduction

Estimations of the backwater zone, i.e. the reach of the riverbed profile over which channel flow is influenced by a body of standing water (Chow, 1959; Paola & Mohrig, 1996) may be used to predict river and delta behavior as a consequence of sea-level change in modern sedimentary environments. Backwater hydraulics control discharge variations and resulting sedimentary architecture in the backwater zone (Lamb et al., 2012; Nittrouer et al., 2012; Chatanantavet et al., 2012; Blum et al., 2013; Chatanantavet & Lamb, 2014; Colombera et al., 2016; Fernandes et al., 2016; Martin et al., 2018; Trower et al., 2018; Ganti et al., 2019; Gugliotta & Saito, 2019) as during low discharge, deposition takes place in the river channel, whereas high discharge leads to drawdown of the water surface to sea level, inducing flow acceleration and bed scouring (Lamb et al., 2012; Nittrouer et al., 2012; Chatanantavet et al., 2012; Chatanantavet & Lamb, 2014). This link between backwater zone and changes in channel morphology holds therefore potential to improve predictive stratigraphic models with application in subsurface reservoir or aquifer analysis, but also geohazards linked to fluvial hydrodynamics.

In modern river systems, the backwater length (Lb) is determined using direct field measurements of bankfull thalweg channel depth and river water elevation (Nittrouer et al., 2011; Gugliotta et al., 2017; Smith et al., 2020). Alternatively it can be estimated indirectly by Lb = h/S, with h is bankfull (thalweg) channel depth and S is slope (Jerolmack, 2009; Chatanantavet et al., 2012; Blum et al., 2013; Ganti et al., 2014, 2016; Hartley et al., 2016; Fernandes et al., 2016; Brooke et al., 2020, 2022; Prasojo et al., 2022), which is also used to estimate backwater length in ancient settings (Colombera et al., 2016; Lin & Bhattacharya, 2017; Kimmerle & Bhattacharya, 2018; Martin et al., 2018; Trower et al., 2018; Lin et al., 2020; van Yperen et al., 2021). However, there is currently no standardized method to measure slope and channel depth, nor consensus on where to measure these variables, for both modern and ancient settings (Fig. 1). This is illustrated by different backwater length estimates for the same modern river resulting from different methods (Table 1) with estimates for the Nile river of 92 km (Prasojo et al., 2022), 120 km (Jerolmack 2009), 254 km (Chatanantavet 2012) and 340 km (Hartley et al., 2016). Additionally, in both modern and ancient settings, ambiguity arises from the use of different water levels (Fig. 1) and whether to use bankfull thalweg, or average channel depth, which consequently impacts resulting backwater length estimates. Average channel depth is obtained differently by different authors; one-half of the maximum bankfull thalweg depth (Bridge & Tye, 2000; Leclair & Bridge, 2001; Holbrook & Wanas, 2014); ii) the average of multiple maximal bankfull measurements (Lin & Bhattacharya, 2017); and iii) the average bankfull depth across a full cross-sectional profile (Long, 2021). Bankfull water level is considered as having the most profound effect on channel forming (Williams, 1978). Therefore, we consider 'bankfull channel depth' equal to 'formative flow depth', the latter being important when assessing changes in sediment distribution and channel morphology as a consequence of changes in flow velocity in the backwater zone (Paola & Mohrig, 1996).

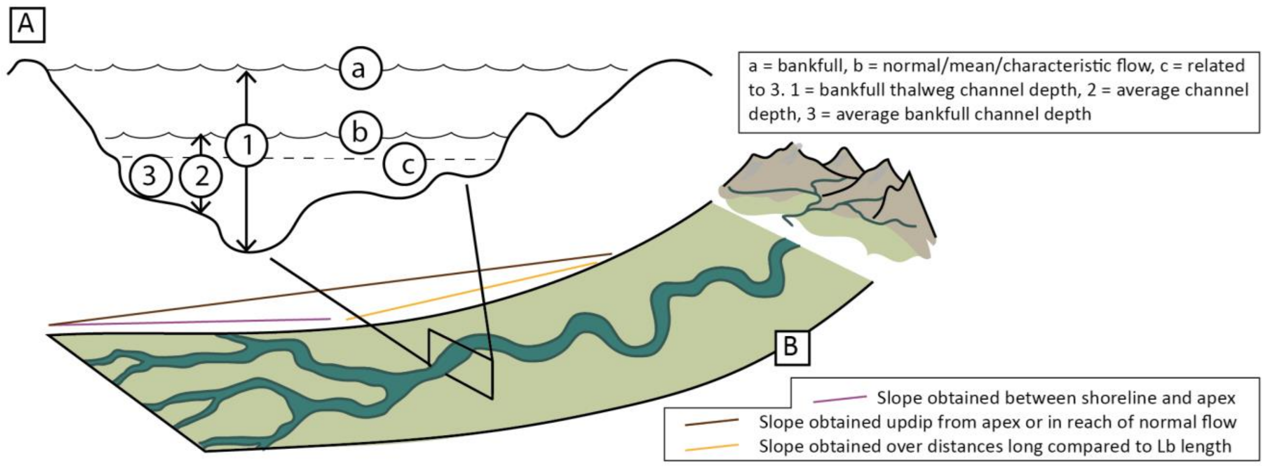

Fig. 1. Summary and depiction of ambiguity and differences in current acquisition methods for backwater length estimates. (A) In cross-sectional view: ambiguity arises from differences in used water level: a) bankfull water level or b) normal/mean/characteristic flow level. Differences in type of channel depth enhance incomparability of backwater estimates; 1) bankfull thalweg channel depth, i.e. deepest point in the channel, at times of water level a, and 2) average channel depth, i.e. linked to water level b, or 3) average bankfull channel depth, which links to level c (which is not a water level) and is obtained differently by different authors (see section 3.2). (B) Along the down-dip transect, the colored lines represent slopes measured over different distances as used in publications addressing backwater estimates in modern river systems (Table 3). Such differences will result in different backwater length estimates. In the modern, channel depth and slope measurements tend to be averaged out over a certain part of the river path, whereas in the ancient, depth and slope estimates are often obtained from a few selected locations.

Given the ambiguity and differences in current acquisition methods, it is crucial to analyze comparability of previously published backwater length estimates and analyze strengths and limitations of the different methods used. Finally, methods to infer the input parameters necessary to estimate backwater length (i.e. channel depth and slope) are numerous, and each have their inherent uncertainties. These uncertainties are commonly not acknowledged and backwater estimates are presented as true estimates, with very few exceptions (Brooke et al., 2020, 2022).

The aims of this paper are: 1) to compile previously applied methods for estimating backwater lengths in both modern and ancient settings and provide an overview of their differences, sources of error, and limitations, 2) to discuss challenges and limitations of collecting input parameters, 3) to propose workflows based on available input data, and unify methods to estimate backwater lengths in both modern and ancient settings, aiming to minimize ambiguity and maximize practicality, 4) to test the proposed workflows on a rock record case study and a modern river system, and 5) to discuss uncertainty factors for each workflow, as well as the shortcomings, applications and recommendations of using the backwater concept.

River	Country	Prasojo et al. 2022	Hartley et al. 2016	Jerolmack 2009	Chatanantavet et al.	Brooke et al. 2022	Nittrouer et al. 2011	Fernandes et al. 2016	Ganti et al. 2014	Gugliotta et al. 2017
Amazon	Brazil	-	1952	-	400	-	-	-	-	-
Brahmaputra	Bangladesh	-	278	70	-	-	-	-	-	-
Danube	Romania	1543	-	125	125	126	-	-	-	-
Ebro	Spain	19	-	30	-	-	-	-	-	-
Magdalena	Colombia	169	-	63	63	63	-	-	-	-
Manitoba	Canada	-	779	5	8	-	-	-	-	-
Mekong	Vietnam, Cambodi	692	-	-	-	-	-	-	-	560
Mississippi	USA	338	842	833	480	488	680	328	-	-
Niger	Nigeria	113	256	-	-	-	-	-	-	-
Nile	Egypt	92	340	120	254	253	-	-	-	-
Orinoco	Venezuela	586	240	200	133	133	-	-	-	-
Paraná	Argentina	-	451	73	295	295	-	-	-	-
Rhine-Meuse	Netherlands	-	-	45	46	45	-	71	-	-
Rhône	France	9	81	148	-	-	-	-	-	-
Volga	Russia	184	-	180	-	-	-	-	-	-
Zambezi	Mozambique	23	72	-	-	-	-	-	-	-
Huange / Yellow	China	-	25	10	-	41	-	-	21-54	-

Table 1. Table listing modern deltas for which the Lb (km) has been estimated in multiple publications. See Fig. 2 for a map view of a selection of these deltas. Note: Lb lengths for the Mississippi river and Paraná river for Jerolmack (2009) are computed based on the values listed in Table 1 in Jerolmack (2009). However, Lb lengths for these rivers are displayed differently on the figures in the same publication.

2. The backwater effect

Adjustments in open-channel flow as a response to the proximity of a body of standing water are called 'backwater effects' and represent a change from normal to non-uniform flow conditions (Paola and Mohrig 1996). The quantity H/S is a length scale that governs the streamwise distance over which these adjustments occur, and was termed 'backwater length' by Paola and Mohrig (1996). This length scale is derived from basic fluid momentum balances in which the Froude number is a critical parameter determining whether or not downstream boundary conditions such as base level can influence upstream hydrodynamics (Parker, e-book):

$$F^2 \left[\frac{H^2 2g}{L}\right] \sim \left[\frac{H^2 g}{L}\right] + HgS + \frac{\tau}{\rho} \qquad (1)$$

Where H is depth, τ is Shear stress, F is the Froude number, g is gravitational acceleration, S is slope and ρ is density. The width of the zone where the Froude number $\ll$ 1 and the water surface slope $\ll$ bed slope, is the backwater length (Paola & Mohrig, 1996; Hajek & Wolinsky, 2012). The change from normal to non-uniform flow conditions matches bankfull thalweg channel bed intersecting with sea level (Nittrouer et al., 2011) and several changes in sedimentary patterns occur downstream of the point where the channel bed drops below sea level (Wright & Parker, 2005; Nittrouer et al., 2011; Blum et al., 2013; Fernandes et al., 2016). Field surveys for the lower Trinity river in east Texas (USA) show that where the median riverbed elevation drops below sea level, the low-flow water depth gradually increases and matches large-scale changes in geomorphology (Smith et al., 2020). Blum et al. (2013) and Fernandes et al. (2016) specifically mention that the backwater length corresponds to the distance over which the scoured channel base is at or below sea level.

3. Backwater length estimates in ancient settings

Multiple methods for determining paleohydraulic parameters applicable to ancient fluvial strata exist and attempts to update these equations using empirical re-evaluation of modern stream data are numerous (Long, 2021). Here we focus particularly on publications estimating backwater length and their methods to obtain slope and channel depth (Table 2).

3.1. Location to measure slope and channel depth

In ancient settings, slope and channel depth estimates are obtained from a few selected locations, which contrasts studies from modern river systems, in which channel depth and slope measurements are occasionally averaged out over a certain part of the river path (Fig. 1, Table 2).

Channel depth and slope are i) 'evaluated upstream in reach of normal flow' (Trower et al., 2018; van Yperen et al., 2021), ii) obtained in 'relatively proximal portions of the paleodelta system' (Kimmerle

& Bhattacharya, 2018; Martin et al., 2018), iii) inferred from the gradient of back-stripped stratigraphic correlation across the full fluvial to marine-shelf profile (Lin et al., 2020) or iv) lack further specification (Table 2). Paola & Mohrig (1996), the foundational paper of the backwater effect, note that 'the keypoint is that the depth, slope and shear stress refer to conditions averaged over distances that are long compared with the backwater length' and that 'the idea is to approximate as closely as possible the measurement of an average depth over a section across a modern river'. Both Kimmerle and Bhattacharya (2018) and Martin et al. (2018) acknowledge that the location used for their channel depth estimates is potentially impacted by non-uniform flow conditions, but reason that – in the proximal reaches of their study case – such effects are likely muted or covered by natural uncertainty in the method itself. Lin et al. (2020) use sample locations from within the backwater zone in the Gallup system but do not comment about a potential influence on the backwater length estimates.

Recommendations: the location to measure slope and channel depth is inherently connected to the selected method to estimate these two parameters, and may depend on the available data (e.g. outcrop extent, coverage of subsurface data set). Slopes generally decrease towards the shoreline as the channel enters the backwater zone, which implies that backwater lengths calculated from slopes obtained within the backwater zone are longer than backwater lengths calculated from slopes obtained updip of the backwater zone, for the same river. We recommend that paleohydraulic analysis should be calculated for normal-flow zone conditions, i.e. landward of the backwater zone (e.g. Fernandes et al., 2016), to allow comparison between normal flow parameters versus paleohydrualic estimates obtained in the backwater zone, in order to evaluate backwater effects on sedimentation patterns. This implies a chicken-and-egg-situation; one needs to select a location to obtain depth and slope to estimate backwater length, but the backwater length is needed to define the upstream limit of non-uniform flow condition, which in turn determines where to sample channel depth and slope. Alternatively, changes in fluvial architectural style could be used to interpret the presence/absence of backwater conditions (van Yperen et al., 2021)), but this implies a causal relationship between the two, which is unwanted in case the effects of backwater processes on sedimentation patterns are to be tested. We therefore recommend an iterative process that narrows the potential backwater length by estimating values at multiple locations until the sample is upstream and therefore in normal-flow conditions, of the most reasonable backwater estimate.

Reference	**Study type**	**Slope measurement location**	**Slope measurement method**	**Channel depth**	**Depth measurement location**	**Depth measurement method**
Colombera et al. 2016	Outcrop, Cretaceous Neslen Formation	No comments	Inferred from the gradient of transgressive surfaces	Bankfull depth	No comments	Maximum bar thickness or cross-strata set tickness
Lin and Bhattacharya 2017	Outcrop, Cretaceous Dunvegan Alloformation	No comments	$\tau*_{bf50} = (d_m S)/(PD_{50})$ = constant *sensu* Holbrook and Wanas (2014) and Trampush et al. (2014)	Bankfull channel depth	No comments	Channel-depth values estimated from multiple methods; fining-upward channel stories, point-bar deposits, lateral-accretion bars, average cross-set thickness, statistics from well-log data. Use of minimum and maximum average value of compiled channel depths.
Trower et al. 2018	Outcrop, Cretaceous Castlegate Sandstone	*"Evaluated upstream in reach of normal flow"*	Slopes were calculated using Shields relation: log S =-2,08+(0,254*logD_{50})-(1,09*logH_{bf}) *sensu* Trampush et al. (2014)	*"Characteristic bankfull flow depth"*	*"Evaluated upstream in reach of normal flow"*	Bankfull depth inferred from bar heights and scour depths measured in a transect along the paleo-flow direction.
Kimmerle and Bhattacharya 2018	Outcrop, Cretaceous Ferron Sandstone	Stratigraphicallly derived slope and estimates based on Holbrook and Wanas (2014). D50 for each valley, within the backwater zone.	D_{50} and bankfull channel depth were used to estimate channel slope, as per the method described by Holbrook and Wanas (2014) and method 1 of Lynds et al. (2014). They also use slope estimates based on long-profile erosional relief of Ferron incised valleys (Zhu et al 2012)	Bankfull channel depth	Within the backwater zone, interpreted to be at the landward end of the backwater zone.	Backwater in their table 5, paleohydraulics in their table 2 and 3. Paleohydraulic analysis based on measured point-bar thickness and cross-set thickness (Mackey and Bridge 1995; Bridge and Tye 2000; Leclair and Bridge 2001; Bhattacharya and Tye 2004; Holbrook and Wanas 2014) compared with estimates directly derived from outcrop exposures, by using rollover geometries in accreting-point-bar deposits as representative of complete bar preservation (Hajek and Heller 2012)
Martin et al. 2018	Subsurface, Triassic Mungaroo Formation	*"Relatively proximal portions of the Mungaroo paleodelta system"*, acknowledging potential influence of non-uniform flow conditions	Using a global dataset that relates particle size (D) and boundary shear stress (τ) from modern rivers (Trampush et al. 2014): $S=\tau/(gH_{ch})$. Produced range of paleoslope estimates to include natural variability in bankfull shear stress.	Characteristic channel depth	*"Relatively proximal portions of the Mungaroo paleodelta system"*, acknowledging potential influence of non-uniform flow conditions	Dune height from cross-set thickness (Paola and Borgman, 1991) and flow depth from dune height (Yalin 1964; Allen 1983) and subsequent syntheses (Leclair and Bridge 2001; Venditti 2013).
Lin et al. 2020	Outcrop, Cretaceous Gallup Sandstone	Regional sequence stratigraphic correlation from fluvial to marine shelf, or fluvial section only. Grainsize samples from both fluvial and terminal distributary channel deposits.	Stratigraphic correlations and numerically; $\tau*_{bf50} = (d_m S)/(PD_{50})$	Bankfull flow depth	From a fluvial channel and two terminal distributary channel deposits.	Bankfull flow depth btained from fully preserved channel stories or from dune-scale cross bedding and bar accretion deposits, using 6-10x average dune height to calculate average channel depth, and dune heigh is 2.9 (± 0.7) x the average cross-set thickness (Leclair and Bridge 2001)
Van Yperen et al. 2021	Outcrop, Cretaceous Dakota Group	*"Evaluated upstream in reach of normal flow"*	$\tau*_{bf50} = (d_m S)/(PD_{50})$	Bankfull flow depth	*"Evaluated upstream in reach of normal flow"*	Bankfull channel depth inferred from completely preserved trunk channel deposits or mean dune height calculated from cross-set thickness (Leclair & Bridge, 2001) from which bankfull paleoflow depths are calculated (Allen, 1982; Best & Fielding, 2019; Bradley & Venditti, 2017)

Table 2. Overview of selected publications addressed in this review and their methods to obtain input parameters to estimate backwater length in ancient settings. Direct quotations in *italic*.

3.2. Channel depth type

A variety of channel depth types have been listed when estimating backwater lengths in ancient settings: bankfull channel depth, bankfull thalweg depth, average bankfull channel depth, characteristic channel depth, and characteristic bankfull flow depth (Fig. 1, Table 2). Only a few publications specify exactly what they mean with their selected channel depth type (Bridge & Tye, 2000; Leclair & Bridge, 2001; Holbrook & Wanas, 2014; Lin & Bhattacharya, 2017; Long, 2021). Moreover, these few cases highlight that usage of the same term does not imply the same understanding and hence application of the selected depth type: 'average bankfull channel depth' has been explained as i) one-half of the maximum bankfull thalweg depth (Bridge & Tye, 2000; Leclair & Bridge, 2001; Holbrook & Wanas, 2014); ii) the average of multiple maximal bankfull measurements (Lin & Bhattacharya, 2017); and iii) the average bankfull depth across a full cross-sectional profile (Long, 2021). Such mixing of terminology definitions and the use of different channel depth types causes confusion and exhibits a source of error. For example, based on a hypothetical dataset consisting of 5 channel depth measurements (10 m, 11 m, 12 m, 13 m, 14 m channel thickness) and a slope of 0.0001 (i.e. 1 m per 10 km), using the average of multiple maximal bankfull measurements (Lin & Bhattacharya, 2017) or one-half of the maximum bankfull thalweg depth (Bridge & Tye, 2000; Leclair & Bridge, 2001; Holbrook & Wanas, 2014) results in backwater lengths of 120 km (i.e. 12 m / 0,0001) versus 70 km (i.e. 7 m / 0,0001), respectively. Note that this example illustrates the different understandings of '*average* bankfull channel depth'. Finally, the – unintended – mixing of terminology is illustrated by publications using the same method to establish channel depth, but using different terms for the channel depth *type* (cf. Martin et al., 2018; van Yperen et al., 2021; Table 2).

Recommendations: when deciding which channel depth type to use for backwater estimates, it is essential to 1) consider the hydrodynamic meaning of the different depth types, and 2) define what the recommended channel type implies, i.e. clarifying the terminology used in order to minimize ambiguity when discussing methods to obtain this parameter. Hydrodynamically, the upstream limit of the backwater zone marks the area where normal flow conditions transition into non-uniform flow (Paola & Mohrig, 1996). This adjustment in flow impacts sediment distribution and hence channel morphology. Adjustments in channel morphology are considered to occur predominantly at bankfull conditions (Williams, 1978) albeit that a range of discharges, rather than a single event magnitude, can determine the morphology and long-term stability of a given channel-reach (Pickup & Warner, 1976; Pickup & Rieger, 1979; Graf, 1988; Surian et al., 2009). Bankfull *thalweg* depth (i.e. the maximum depth across a cross-sectional channel profile, related to bankfull flow conditions, Fig. 1) can be directly measured in outcrop studies, based on preserved single story thickness, provided that such fining upward channel successions are encapsulated in overbank deposits (Bridge & Tye, 2000; Hajek & Heller, 2012; Holbrook & Wanas, 2014; Milliken et al., 2018; Long, 2021). In subsurface core (or well log) data, similar successions provide bankfull depth, albeit that the well might not intersect the deepest part of the channel. Finally, for reasons listed above, any type of 'average' channel depth is a recipe for confusion as there are different understandings of how to achieve the average (cf. Bridge & Tye, 2000; Leclair & Bridge, 2001; Holbrook & Wanas, 2014; Lin & Bhattacharya, 2017; Long, 2021). Taking all the above into consideration, we recommend using bankfull thalweg depth, i.e. the maximum depth across a cross-sectional channel profile, as this represents bankfull flow conditions which are considered to represent channel forming conditions. Additionally, bankfull thalweg depth is easily obtained in the field, and the term itself minimizes ambiguity as *maximum* depth is unambiguous and therefore pragmatic and consistent.

3.3. Methods to obtain bankfull thalweg channel depth

Methods used to infer channel depth for backwater length estimates in ancient settings are twofold: i) direct measurements in the field, such as from maximum scour depth, maximum bar height and point-bar deposits, and ii) empirically by estimating flow depth from dune height from mean cross-set thickness (Table 2). Comparing empirically reconstructed flow depth with direct field measurements shows consistency between these two methods (Kimmerle & Bhattacharya, 2018; Lyster et al., 2021; van Yperen et al., 2021). However, none of the publications in Table 2 take a compaction factor into account.

Recommendations: A correction for burial compaction should be performed, either after obtaining mean cross-set thicknesses to be used for empirically estimating channel depth or onto thicknesses derived from direct field measurements of preserved single-story channel deposits. Ideally, the compaction factor should be estimated based on thin-section data. If not available, a compaction factor of 1.1 is commonly used (Holbrook & Wanas, 2014; Long, 2021), but it is important to acknowledge that the likely range is between 1.0 and 1.69 (Long, 2021).

For direct outcrop measurements, we recommend inferring bankfull thalweg channel depth from completely preserved single-story trunk channel deposits. Other channel elements often used to obtain channel depth, such as barforms and large-scale planar cross-strata, typically represent less than bankfull thalweg depth (Long, 2021, and references therein). Note that thalweg fill deposits, if present, are not part of the channel fill story thickness, but rather represent localized heightened energy related to cut-and-fill events (Holbrook & Wanas, 2014). Therefor these should be excluded when measuring preserved single-story channel thickness.

When estimating flow depth empirically, from dune height via mean cross-set thickness, we recommend using the relation of Leclair and Bridge (2001) to infer mean dune height, h_d, from mean cross-set height, $h_{xs\text{-}mean}$:

$$h_d = 2.9(\pm 0.7)h_{xs\text{-}mean} \quad (2)$$

Cross-set thicknesses should be measured on through cross-bedding and/or tabular cross-bedding, as these are sedimentary structures from bedforms indicative of bedload transport (Rubin & Carter, 1987). A newly established relationship between maximum ($h_{xs\text{-}max}$) and mean cross-set height ($h_{xs\text{-}mean} = 0.7(\pm 0.01)h_{xs\text{-}max}$) allows collection of maximum cross-set thickness in the field rather than height distributions of individual cross-sets (Fig. 5A *in* Lyster et al., 2021). Maximum cross-set measurements should be collected from the lowermost bedforms, as these are representative of formative flow depth.

To scale mean dune height (h_d) to formative flow depth (H), we recommend using Bradley & Venditti's (2017) scaling relationship, based on 382 field observations, where:

$$H = 6.7h_d \quad (3)$$

A reevaluation of this relationship (Long, 2021) suggests an adjustment in which they disregard the scaling break in dune height between deep and shallow flows as documented by Bradley & Venditti (2017). In fact, Bradley & Venditti (2017) already point out that this scaling break is not apparent when h_d is used as the independent variable and therefore also exclude this from their analysis. The only difference underlying the two different scaling relationships between mean dune height and formative flow depth (cf. Bradley & Venditti, 2017; Long, 2021) is the data included in the analyses: Bradley & Venditti (2017) exclude flume experiments, as '*most of the flume data plot above the H/6* (Yalin, 1964) *scaling relation'* and '*Dunes in natural channels are responsible for the features preserved in the rock record and the inclusion of data from idealized flume experiments may not be appropriate.'* We support this reasoning and therefore recommend using equation 3 rather than the adjustment suggested by Long (2021) when inferring channel depth empirically from mean cross-set thickness. However, we prefer using bankfull thalweg channel depth from fully preserved channel story thickness (see section 6.2.), as this provides smaller uncertainty ranges than bankfull thalweg channel depth inferred empirically from average cross-set thickness (see section 4).

3.4. Methods to obtain slope

Methods used to obtain slope for backwater length estimates in ancient settings are two-fold: i) empirically, based on its relation to grain size and ii) based on stratigraphic correlations (Table 2). Kimmerle & Bhattacharya (2018) and Lin et al. (2020) use both these methods and show that empirically derived slopes are approximately five times (Lin et al., 2020) and up to ten times (Kimmerle & Bhattacharya, 2018) smaller than stratigraphically derived slope estimates. This significantly impacts subsequent backwater length estimates. The empirical derived slopes are based on the relationship between grain size and Shields stress:

$$S = RD_{50}\tau^* / H \qquad (4)$$

where S is slope, R is the dimensionless submerged specific gravity of sediment in water with 1.65 for quartz, τ^* is the Shields stress, and H is the flow depth (Shields, 1936; Parker et al., 2007; Holbrook & Wanas, 2014). An important note is that this method based on shear stress, submerged dimensionless density and D50 uses *mean* bankfull flow depth, and not bankfull *thalweg* flow depth (Holbrook & Wanas, 2014). Therefore, if a proxy used for channel depth represents bankfull thalweg depth (e.g. fully preserved channel story thickness measured on an outcrop) a conversion to mean bankfull flow depth will need to be made before inserting this channel depth in the equation (see equation 8 in 4*.3 Channel depth type).*

Although not used for backwater estimates, Lyster et al. (2021) estimated slopes for paleohydraulics based on equation 4 and equation 5:

$$LogS = \alpha_0 + \alpha_1 logD50 + \alpha_2 logH \quad (5)$$

where *H* is bankfull channel depth *and* the constants are given by α_0 = -2.08 ± 0.036, α_1 = 0.254 ± 0.016, and α_0 = -1.09 ± 0.044 (Trampush et al., 2014). Their slope estimates based on equation 4 are up to a factor of 2 greater than slop estimates based on equation 5.

Recommendations: In general, there is yet no clear path to resolve river gradients in ancient deposits, as sinuosity, climate zone, and grain size all play a significant role and many stages of calculation may introduce potential errors, regardless the method used (Long, 2021). It is beyond the purpose of this paper to provide a full review of methods to estimate slope. According to Long (2021), empirical relationships for slope estimates with equation 4 (Shields, 1936; Parker et al., 2007; Holbrook & Wanas, 2014; Trampush et al., 2014) generally plot lower than the observed slope. They therefore recommend using a different relationship, i.e. $S = 0.0239 (D_{50}/d_{bf})^{0.4763}$. However, based on the following we propose to use equation 4 regardless; i) the relationship proposed by Long (2021) has an uncertainty factor of 27 (see Supplemental Text S3) whereas equation 4 has an uncertainty factor of 2 (Holbrook & Wanas, 2014), ii) most streams have excess energy than what is reflected by the grain size, which explains the underestimation of slopes based on equation 4 (Shields stress), iii) both equations require similar data collection efforts as they both utilize grain size samples as input parameter. We recommend to use the empirical relationship based on Shields stress (i.e. equation 4) as this has the least uncertainty. Key is to perform grainsize analysis on a representative sample for bedload transport at times of formative (bankfull) discharge. We recommend to avoid sampling lag deposits at the channel base as they may represent localized heightened energy related to cut-and-fill events (Holbrook & Wanas, 2014) but rather sample the lowest bedform representative for bedload transport. Bedforms positioned higher within the individual channel deposit are best avoided as they are more likely to record infill processes. Additionally, for grain size analysis we recommend using a laser particle size analyzer after rock sample disaggregation rather than thin section analysis, as the first measures silt and clay portions more accurately (Brooks et al., 2022).

If grain size is not available, slope can be based on bankfull channel width (w_{bf}) using Long (2021):

$$S = 0.0341 \times w_{bf}^{-0.7430} \qquad (6)$$

with W_{bf} is bankfull channel depth. Bankfull channel width can be directly measured in the field albeit that channel widths should be corrected for channel elements from outcropping bodies cut at any angle to cross-stream direction.

4. Backwater length estimates in modern river systems

Existing methods to obtain backwater estimates in modern river systems are compiled from fourteen publications (Table 3) and are basically twofold; i) direct assessments of the intersection between riverbed and sea level, and ii) indirect estimate by obtaining input parameters river depth and slope and applying $L_b = h/S$ with L_b is backwater length, h is river depth, and S is slope. Backwater effects are also commonly studied in the field of engineering (Csiki & Rhoads, 2010; Maselli et al., 2018; Liro, 2019; Liro et al., 2020; Amarnath & Thatikonda, 2020), where the backwater zone is a river section upstream of a river dam reservoir that is inundated during reservoir stages higher than the normal or average (Liro, 2019), characterized by backwater and drawdown surface water profiles associated with varying low-discharge and high-discharge events (Maselli et al., 2018). In this study, and particularly this section, we focus on backwater length estimates in coastal river systems and unrelated to river dams.

4.1. Location to measure slope and channel depth

In modern river systems, slope and channel depth measurements are often averaged out over a certain part of the river path to obtain the input parameters for backwater length estimates (Fig. 1, Table 3).

Reference	Study type	Slope measurement location	Slope measurement method	Channel depth type	Channel depth measurement location	Depth measurement method
Paola and Mohrig 2006	Ancient & modern rivers	*"depth, slope and shear stress refer to conditions averaged over distances that are long compared with backwater length"*	Determine average and median values for depth and grainsize. Subsequently calculate a single slope estimate.	Channel depth	*"depth, slope and shear stress refer to conditions averaged over distances that are long compared with backwater length"*	*"… measuring as many depth indicators as possible over the oucrope area."*
Jerolmack 2009	Mathematical model and the Mississippi and Rhine-Muse rivers	*"S is the river slope upstream of the delta"*	*"Hydraulic and geometric parameters, compiled from literature"*	Channel depth. No specification, but Fig. 7 suggests it might be bankfull	No comments	No comments - Fig 8 indicates channel depth from Jerolmack and Mohrig (2007). We cannot retrieve depth from Jerolmack and Mohrig (2007).
Nittrouer et al. 2011	Mississippi river	Slope is measured for the lower 1050 river kilometers.	Slope is measured from low, moderate and high water level surface elevation at 18 gauge stations.	Thalweg depth	Lower 1050 river kilometers	Hydrographic river bed survey (from Harmar and Clifford, 2007).
Chatanantavet et al. 2012	2D model and 9 modern river deltas	No comments about location.	*"The channel slope for each river was calculated from existing literature"*	Characteristic flow depth = normal flow depth	*"Upstream of the backwater zone"*	Characteristic flow depth $h_c = (C_f Q_c^{\,2} / g w^2 S)$^1/3 (*sensu* Parker, 2004). C_f = bed friction coefficient, Q_c = characteristic water discharge, w = channel width, g = gravitational acceleration, S = slope.
Blum et al. 2013	Review	Slopes depicted in Fig 4B but without reference, no in-text comments	Slopes depicted in Fig 4B but without reference, no in-text comments	*"typically bankfull channel depth"*	No comment. Depths depicted in Fig 4B but without reference.	No comment. Depths depicted in their Fig. 4B but without reference.
Ganti et al. 2014	Huanghe river	*"Channel bed slope in the lower Huanghe reaches, from Luokou to Lijin"*. Upstream of backwater zone.	Range based on slopes measured the last 70 years. Method not mentioned.	Bankfull flow depth	One location, i.e. Lijin, 120 km from the shoreline. Estimated backwater length is 21-54 km.	Based on historical data published in previous publications.
Hartley et al. 2016	13 modern rivers, single thread, low gradient	*"…..between the bankfull elevation at the apex and te shoreline of each delta and cross-checked with the literature to ensure consistency."*	Channel bankfull slope from Digital Elevation Models from Shutle Radar Topography Mission	*"h_f is flow depth (typically bankfull channel depth)"*	*"for most examples include an average depth of the apex-shoreline length. Where this was not available, reliable depth measurements for portions of the river close to the apex were used"*	Published information or *"reliable depth measurements for portions of the river close to the apex were used"*
Ganti et al. 2016	Scaled physical experiments* and 8 modern delta rivers from Chatanantavet et al 2012**	*"within the normal-flow zone"* / no comments**	**no comments	Normal-flow depth* / characteristic flow depth**	*"within the normal-flow zone"** / no comments**	*"Measured flow depth computed by differencing the water surface profile and the bed surface profile within the confined portion of the experimental facility"** / formula based on discharge (Parker)**
Fernandes et al. 2016	Mississippi and Rhine	Estimated in the normal flow reach (Mississippi river), more than one channel depth above mean sea level and upstream of backwater zone (Rhine river)	Water surface gradient in the normal flow reach (Mississippi river), channel belt gradients based on highest elevation of bar sand, taking into account sinuosity (Rhine river).	Mean channel depth	Rhine river: no comments, Mississippi river: upstream of CBK 300.	Low, intermediate and high values of mean normal flow depth were acquired from depths of filled oxboy lakes (Mississippi river) or channel belt thickness (Rhine river)
Gugliotta et al. 2017	Mekong river	Not applicable - (Lb is taken where sea level intersects the riverbed profile)	Not applicable - (Lb is taken where sea level intersects the riverbed profile).	Riverbed - no further comments (irrelevant as Lb is taken where sea level intersects the riverbed profile)	Lower 750 river kilometers, estimated backwater length is 560 km.	Riverbed elevations measured at 1-km intervals from hydrological atlases (Mekong River Commission and Ministry of Transport of Vietnam & Cambodia, in Oketani and Haruyama 2011)
Brooke et al. 2020	Steep rivers, Madagascar	Evaluated in the 25 km bin immediately upstream of the avulsion sites	Measured from elevation change every 5 km and binned into 25 km segments, based on digital elevation model from Shutle Radar Topography Mission 2000.	Bankfull flow depth	Evaluated upstream of the avulsion site	*"…using the empirical bankfull Shields stress relation (Trampush et al., 2014) and the threshold channel theory for alluvial rivers (Dunne & Jerolmack, 2018). These independent methods yielded consistent bankfull flow depth values."*
Smith et al. 2020	Lower Trinity River, Texas	Based on an average across the lower 110 river kilometers (from Phillips et al., 2005)	From channel thalweg elevations (Phillips et al. 2005)	Average channel depth	Based on an average across the lower 110 river kilometers, estimated backwater length is 60 km.	From channel cross-sections from channel surveys (in Phillips et al., 2015)
Brooke et al. 2022	Avulsion sites on modern rivers	No comments	From previous publications if available. If not, from the 15arc-sec resoltion HydroSHEDS DEM (Yamazaki et al. 2011) or based on channel-floodplain slope from a STRM and AW3D30 composite.	Bankfull flow depth	Upstream of the avulsion site	From previous publications if available. If not, then $h_{bf} = Max[0.5Q^{0.3}, 1.0]$. Q = long-term average water discharge (Trampush et al. 2014; Cohen et al. 2014). Validity of this equation was tested by comparing with bankfull flow depth estimates based empirically on bankfull Shields stress criterion.
Prasojo et al. 2022	105 modern deltas	No comments about location	Digital Elevation Models from Shutle Radar Topography Mission: Slope is calculated from the water elevation profile along the centerline of the main distributary channel.	Characteristic flow depth	"Qc (characteristic water discharge) is taken as close to the upstream limit of the delta as data availability allows"	Characteristic flow depth $h_c = (C_f Q_c^{\,2} / g W_{av}^{\,2} S)$^1/3 (*sensu* Parker, 2007). C_f = bed friction coefficient, Q_c = characteristic water discharge, W_{av} = channel width, g = gravitational acceleration, S = slope.

Table 3. Overview of selected publications addressed in this review and their methods to obtain input parameters to estimate backwater length in modern river systems. Direct quotations in italic.

Slope for backwater length estimates is obtained along contrasting segments of the river path; i) in normal flow reaches (Fernandes et al., 2016), ii) measured across 25 km upstream of the avulsion site (Brooke et al., 2020), iii) measured 'upstream of the delta' (Jerolmack, 2009), iv) measured 'between the bankfull elevation at the delta apex and the shoreline' (Hartley et al., 2016) or v) lack further specification (Table 3). Both Jerolmack (2009) and Hartley et al. (2016) list backwater length for a set of the same deltas, in which estimates by Hartley et al. (2016) are consistently longer than those by (Jerolmack, 2009) (Table 1, Fig. 2). Their different choices for the location to obtain river slope partly explain this; delta plain slopes (Hartley et al., 2016) tend to be lower than river slopes upstream of the apex (Jerolmack, 2009), in addition to channel depths listed by Hartley et al. (2016) being thicker (Supplemental Table S1 and S2). A continuous profile over distances longer than the backwater length is used by Paola & Mohrig (2009), Nittrouer et al. (2011) and Gugliotta et al. (2017). Because river surface elevation profiles asymptotically approach the relatively fixed water surface elevation of the receiving basin (Chow, 1959), obtaining slope from different segments results in different steepness which may lead to backwater lengths with up to a factor 2 difference, based on results from the Mississippi river (Fig. 3A, Supplemental Table S3A).

Channel depth for backwater length estimates has previously been obtained along different segments of the river profile as well: i) 'upstream of the backwater zone' (Chatanantavet et al., 2012), ii) 'evaluated upstream of the avulsion site' (Brooke et al., 2020, 2022), iii) 'as close to the upstream limit of the delta as data availability allows' (Prasojo et al., 2022), at iv) one location only (Ganti et al., 2014), v) across long stretches of the river path (Nittrouer et al., 2011; Gugliotta et al., 2017) or vi) lack further specification (Table 3). Studies in which channel slope and depth are obtained from datasets that cover the river path continuously over stretches longer than the backwater length are few (Nittrouer et al., 2011; Gugliotta et al., 2017). This reflects the efforts (e.g. bathymetric survey of hundreds of river km) needed to obtain such continuous riverbed profiles. Obtaining channel depth from different segments of the river may lead to ¬15% difference in backwater length calculation, based on results from the Mississippi river (Fig. 3B, Table S3B).

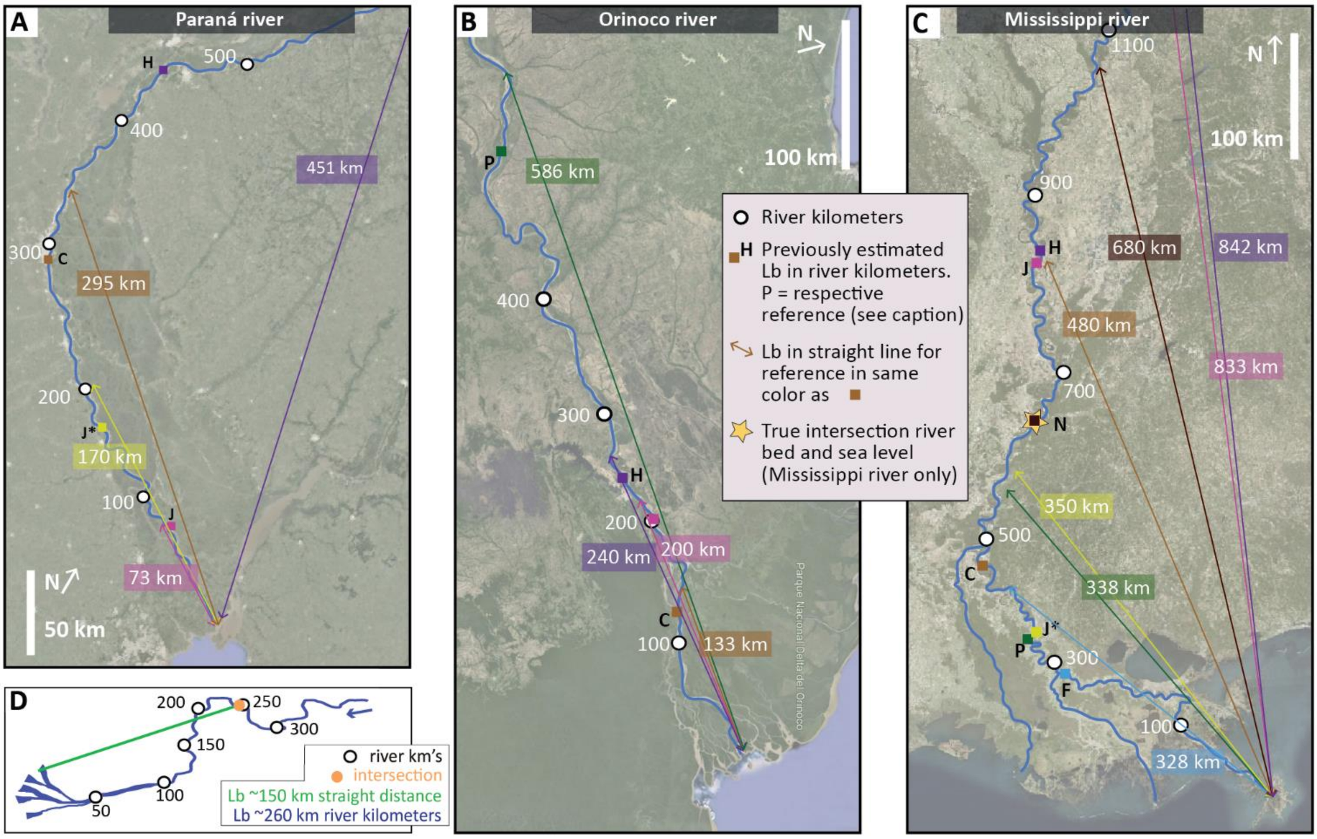

Fig. 2. Backwater length estimates by different authors for the Paraná river (A), Orinoco (B) and Mississippi river (C). Landward extend of estimated backwater length based on Lb= h/S is displayed both in river km (■) and straight-line distances. Each reference has its own color that is used for both ■ and the straight line. Note the difference between approaching h/S trigonometrically (i.e. with straight-line distances) or using river km. J = Table 1 in Jerolmack (2009), J* = Fig. 9 and 14 in Jerolmack (2009), C = Chatanatavet et al. (2012); F = Fernandes et al. (2016); H = Hartley et al. (2016), P = Prasojo et al. (2020). See table 1 for Lb estimates. Backwater lengths in km as previously published are labeled onto the distances depicted as straight lines. (D) Annotation of the backwater length (Lb) in km varies among publications; in river km (blue) or a straight line to the coast (green), which gives different backwater length estimates. Intersection of the riverbed with sea level occurs at the brown circle. Subsequently, the backwater length (Lb) is ~150 km (i.e. straight line to the coast, in green) or ~260 km (i.e. river km, in blue).

Recommendations: Riverbed profiles typically show significant local variation and water surface slopes steepen in landward direction, inherent to the typical graded river profile (Mackin, 1948). Subsequently, it is impossible that slope and depth estimates from only one single location provide representative parameters. Therefore, the preferred method to estimate backwater length in modern rivers is to use datasets with channel slope and depth covering the river path over long distances in order to identify where the riverbed elevation intersects sea level (Nittrouer et al., 2011; Gugliotta et al., 2017). By doing so, the locally irregular riverbed profile is averaged over a longer section, and subjectivity and ambiguity in obtaining slope and depth from one or a few selected locations or a certain section of the river path, is minimized. However, datasets with long profile river depths are scarce and will limit the application of such 'intersection method'. See section 5 for further discussion.

4.2. Backwater length estimates

Backwater length is measured along the river centerline in river km (Nittrouer et al., 2011; Blum et al., 2013; Smith et al., 2020) or as a straight distance to the coastline (Jerolmack, 2009, and in ancient settings), after defining where the riverbed intersects sea level or deriving it from h/S. However, most publications do not elaborate on how they measure this distance. Yet, differences can be significant depending on river sinuosity (Fig. 2D). For instance, using an intersection method to estimate backwater length for the Mississippi river, Nittrouer et al. (2011) measures ~680 river km between the coastline and where the thalweg channel depth intersects sea level, compared to ~370 km when taking a straight line (Fig. 3C). For a hypothetical river with a sinuosity index of 2, the point on the map calculated as the upstream limit of the backwater length will be twice as far away from the coastline when using straight line compared to measuring in river km.

Recommendations: the most important is that authors specify the distance annotation they use (i.e. river km or straight line from intersection to river mouth) and to be aware that the use of different methods should be taken into account when comparing backwater estimates from different publications. We exemplify the trigonometric approach (i.e. using a straight line to depict backwater lengths resulting from Lb = h/S) with the Mississippi river (Fig. 2). This illustrates how plotting straight line distances for previously estimated backwater lengths results in upstream limit of backwater zones that are several hundred river km upstream of the actual riverbed intersection with sea level. Based

Section 4.1. Location to measure slope and channel depth, Section 4.2. Backwater length estimates

A Slope

Input location	Selected reference*	Input parameters based on bankfull discharge	depth (m)	Slope	Backwater length (km)
1. Between apex and shoreline	This study, following Hartley et al. 2016	19 m elevation at 490 river km 0 m elevation at 0 river km	31	3.88E-05	799
2. Normal flow reach	This study, following Fernandes et al. 2016	53 m elevation at 1050 river km 26 m elevation at 650 river km	31	6.75E-05	459
3. Upstream of avulsion site, across 25 km	This study, following Brooke et al. 2020	20 m elevation at 515 river km 19 m elevation at 490 river km	31	4.00E-05	775
4. Distances long compared to backwater length ♦	This study, following Paola and Mohrig 2009 ♦	54 m elevation at 1050 river km 0 m elevation at 0 river km	31	5.14E-05	603

(Input: first four columns; Output: Slope, Backwater length)

B Depth

Input location	Selected reference*	Slope	Channel depth (m)	Backwater length (km)
Upstream of backwater zone	This study, following Chatanantavet et al. 2012	6.75E-05	26	385
Upstream of avulsion site	This study, following Brooke et al. 2020	6.75E-05	27	400
As close to the upstream limit of the delta as data availability allows	This study, following Prasojo et al. 2022	6.75E-05	29	430
Apex	This study, following Ganti et al. 2004	6.75E-05	29	430
Average depth over distances long compared to backwater length	This study, following Paola and Mohrig 2009	6.75E-05	31	459
Continuously, lower 1050 river kilometers	Nittrouer et al. 2011	6.75E-05	along river path	680**

(Input: first three columns; Output: Channel depth, Backwater length)

C

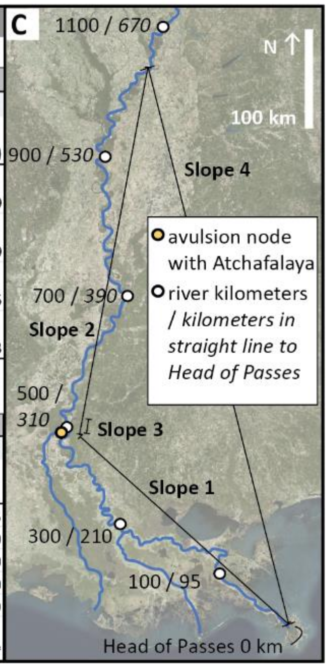

D **Section 4.3. Channel depth type**

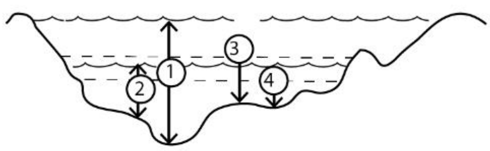

Type of channel depth	Selected reference*	Slope	Channel depth (m)	Backwater length (km)
1. Bankfull thalweg	Nittrouer et al. 2011	6.75E-05	31	459
2. Average depth (equals mean flow depth)	This study, following Bjerklie et al. 2018	6.75E-05	21	419
3. Average bankfull	This study, following Long 2021	6.75E-05	23	468
4. Average bankfull	This study, following Bridge & Tye 2000	6.75E-05	15.5	310

(Input: first three columns; Output: Channel depth, Backwater length)

F **Section 4.5. Methods to obtain slope**

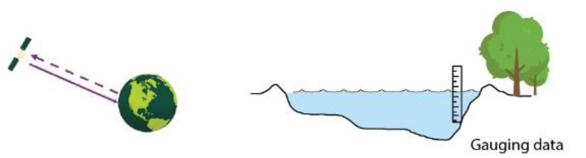

Input data	Selective reference*	Channel depth (m)	Slope	Backwater length (km)
Gauging data: water elevation profile	Fig 2 in Nittrouer et al. 2011	31	6.75E-05	459
Digital elevation model	Following Hartley et al. 2016	31	8.50E-05	365

(Input: first three columns; Output: Slope, Backwater length)

E **Section 4.4. Methods to obtain bankfull thalweg channel depth**

Type of channel depth	Selected reference*	Input parameters	Slope	Channel depth (m)	Backwater length (km)
Direct; riverbed survey	Nittrouer et al. 2011	River bed profile	6.75E-05	along river path	680**
Shields stress	This study - Mississippi river (used in Brooke et al. 2020 for rivers in Madagascar)	$\tau^*_{bf50}=(d_m S)/(P D_{50})$. D_m = mean bankfull channel depth, S = slope = $6.75*10^{-5}$, P = submerged dimensionless density = 1.65 g/cm^3, D_{50} = average grainsize for lowermost portion of the channel = 280 µm, τ_{bf50}= Shields number for dimensionless shear stress = 1.86. The resultig mean bankfull chanel depth (15 m) needs to be converted to obtain bankfull thalweg channel depth with equation 7.	6.75E-05	17	256
River discharge	Prasojo et al. 2022	characteristic flow depth $h_c = (C_f Q_c^2 / g W_{av}^2 S)$^1/3 (*sensu* Parker, 2007). C_f = bed friction coefficient = 0.002, Q_c = characteristic water discharge = 33385 m^3/s, W_{av} = channel width = 669 m, g = gravitational acceleration = 9.8 m/s^2, S = slope = 6.75*10-5.	6.75E-05	20	290
Channel deposits	Fernandes et al. 2016	Filled oxbow lake deposits	6.75E-05	21	311
Literature	Hartley et al. 2016	Published information or *"reliable depth measurements for portions of the river close to the apex were used"*	6.75E-05	25	500

(Input: first four columns; Output: Channel depth, Backwater length) on this, in addition to the omission of large-scale changes in river course if using a straight line and a trigonometric approach, we recommend to use river km (Fig. 2D).

Fig. 3. Error sources and equivocal definitions of input parameters and their impact on backwater length estimates; Mississippi river as an example. This figures assess all aproaches of obtaining input parameters (i.e. channel depth and slope) to estimate backwater length based on Lb = h/S. Different resulting backwater lengths result from obtaining input parameters in various ways. If the approach aims to obtain the parameter 'depth', then a representative value for the parameter 'slope' is kept constant to allow comparison among the resulting backwater length estimates, and vice versa. A slope of $6.75*10^{-5}$ is representative as this resembles the water surface slope of the Mississippi river in the normal flow reach at bankfull stage (Nittrouer et al., 2011). The Mississippi apex and avulsion site is around 490 river km upstream (Chatanantavet et al., 2012). When multiple publications have applied the same method, then a selected reference is listed. (A) Impact of using different segments of a river system to obtain slope. Channel depth is kept constant. Note how slope obtained between apex and shoreline gives the longest backwater length. Location 1-4 are depicted in C. ♦It is unclear whether Paola & Mohrig (1996) include the lower reaches of a river system. (B) Impact of using different segments of a river system to obtain channel depth. Slope is kept constant. **Note how all estimates result in backwater lengths shorter than with the intersection method by Nittrouer et al. (2011). (C) Southern Louisiana and Mississippi river. The yellow circle indicates the apex and avulsion node with Atchafalaya river. White circles depicted with a 200 river-km spacing. Straight-line distances (in Italics) to Head of Passes are significantly shorter than distances measured in river km. (D) Impact of different *types* of channel depth for Mississippi river and how this results in different channel depths and backwater length (Lb) estimates. Backwater lengths calculated based on Lb = h/S and we use a slope of $6.75*10^{-5}$ is for each Lb estimate. (E) Impact of different methods to obtain or infer bankfull thalweg depth for Mississippi river and how this results in different channel depths and backwater length estimates. Resulting backwater lengths vary between 256 km and 680 km. (F) Obtaining slope estimates from either digital elevation models or gauging data at bankfull stages gives different results for Mississippi river in normal flow reach. We use a depth of 31 m for each Lb estimate (Fig. 2 in Nittrouer et al., 2011), to illustrate how different slope estimates impact the resulting backwater length. See Table 1 and Supplemental text S1 for additional explanation for A-F.

4.3. Channel depth type

A variety of channel depth types has been listed when estimating backwater lengths in modern river systems: i) characteristic flow depth, ii) normal flow depth, iii) bankfull flow depth, iv) average channel depth, and iii) channel depth without further specifications (Fig. 1, Table 3). Fernandes (2016) estimates backwater length for low, intermediate and high values of mean normal flow depth. Few publications specify exactly what they mean with their selected channel depth type. In modern rivers, mean flow depth and bankfull thalweg channel depth typically differ a factor ¬1.5 (Bjerklie et al., 2018). This implies that, on a hypothetical river with a slope of 10^{-4} (i.e. 1 m per 10 km), using a bankfull thalweg depth of 12 m or a mean flow depth of 8 m (a factor -1.5 difference) results in a backwater length of 120 km (i.e. 12 m / 0.0001) or 80 km (i.e. 8 m / 0.0001), respectively. When utilizing the Mississippi river as an example, bankfull thalweg depth (i.e. 31 m) and average bankfull depth (i.e. 15.5 m, following Bridge & Tye (2000) who consider average bankfull depth as one-half of the maximum bankfull thalweg depth) results in a backwater length of 459 km or 310 km, respectively (Fig. 3D, Table S3C).

Recommendations: the mixing of terminology definitions and the use of different channel depth *types*, is a source of error when estimating backwater length in modern river systems. When deciding which channel depth type to use, it is essential to 1) consider the formative conditions for channel morphology, and 2) clarify the used terminology in order to minimize ambiguity when discussing methods to obtain this parameter. Channel formative discharge can be considered to coincide with bankfull discharge (Williams, 1978), although it is apparent that there is a range of discharges, rather than a single event magnitude, determining the morphology and long-term stability of segments of the river long profile (Pickup & Warner, 1976; Pickup & Rieger, 1979; Graf, 1988; Surian et al., 2009).

To be clear on the definition of the selected channel depth type, bankfull *thalweg* channel depth represents the deepest part of a channel cross section and thereby minimizes confusion, contrasting 'average bankfull depth', or just 'bankfull depth' that have been used in different ways previously (see also section *3.2 Channel depth type*). Additionally, this deepest part is important for channel hydraulics that control eventual channel morphology. Obviously, local deep scour holes should be excluded as these may exceed thalweg depth by a factor of five (Carey & Keller, 1957). We therefore recommend using bankfull thalweg channel depth as the unit to calculate backwater estimates, as this represents formative flow conditions and minimizes confusion.

4.4. Methods to obtain bankfull thalweg channel depth

Channel depth for backwater length estimates in modern river systems can be measured directly from riverbed surveys (Nittrouer et al., 2011; Gugliotta et al., 2017; Smith et al., 2020) and from channel deposits (Fernandes et al., 2016) (Table 3). Alternatively, the inference of channel depth as an unknown from other known parameters has been done by using empirical relationships based on Shields stress using grain size (Brooke et al., 2020) or river discharge (Chatanantavet et al., 2012; Prasojo et al., 2022). Lastly, a few publications do not specify their methods to obtain channel depth (Table 3). Application of these different methods on the Mississippi river and with a constant slope, shows that resulting backwater lengths vary between 256 and 680 km, which equals a factor 2.6 difference (Fig. 3E, Table S3D).

Several publications list channel depth for the same rivers (Table 1, Supplemental table 1). Among these, data published by Hartley et al. (2016) and Prasojo et al. (2022) allow for comparison of channel depth from seven rivers based on a) an average depth over the apex-shoreline length but without a specified method (Hartley et al., 2016) and b) inferred from empirical relationships with river discharge following (Parker, e-book; Prasojo et al., 2022). Resulting channel depths are shallower based on the empirical discharge relationships for six out of seven rivers (Supplemental table 1). Chatanantavet et al. (2012) used the same discharge-based empirical relationships to estimate channel depth and analyzed five rivers also present in the dataset of Prasojo et al. (2022), of which three rivers have a shallower channel depth than listed in Prasojo et al. (2022), despite using the same methodology (Supplemental table 1). A limitation of discharge-based empirical relationships is its dependence on the location of gauging stations, and the conversion needed to calculate characteristic water discharge from monthly discharge records. Channel belt depth (Fernandes et al., 2016) provides a similar depth as obtained by others (Chatanantavet et al., 2012; Prasojo et al., 2022) for the Mississippi river and deeper channel depth for the Rhine-Muese river (Supplemental table 1). Channel depths listed in Jerolmack (2009) cannot be used for further comparison as it is unclear how these depth estimates were obtained (Table 1 and 3).

Recommendations: We consider riverbed surveys resulting in absolute heights of the riverbed to be the most accurate channel depth information, as no data conversion is needed to obtain bankfull thalweg depths and it averages the locally irregular riverbed profile over a longer section.

When using river bed bathymetry, or Shields' empirical relationship providing average channel depth, it is important to account for seasonal river level fluctuations and recalculate to bankfull conditions, if needed. For this, we recommend using:

$$D_{bf} = 1.502 \times d_{mf}^{0.9603} \qquad (7)$$

with d_{bf} is bankfull thalweg channel depth, d_{mf} is mean flow depth, and n= 6151 (Long et al., 2021. Note; Long et al., 2021 use $d_{max}$is story thickness x compaction factor for bankfull thalweg channel depth and d_{bf} for 'average depth'. We believe the latter refers to mean flow depth as the source data for this equation is in Bjerklie et al. (2018) who use mean flow depth and maximum depth.

Alternatively, bankfull thalweg channel depth can be estimated from channel width by using:

$$w_{bf} = 16.872\ d_{bf}^{1.169} \qquad (8)$$

with d_{bf} is bankfull thalweg channel depth and W_{bf} is bankfull channel width. Channel width can be measured on satellite imagery.

Finally, bankfull thalweg channel depth can be inferred based on the empirical relationship with discharge and bed friction coefficient (Parker et al., 2007):

$$dbf = (\frac{CfQc2}{gWav2S})^{1/3} \qquad (9)$$

with d_{bf} is bankfull thalweg channel depth, C_f is bed friction coefficient, Q_c is the characteristic water discharge, g is the gravitational acceleration, W_{av} is channel width and S is slope.

4.5. Methods to obtain slope

Methods to obtain slope for backwater length estimates in modern river systems are predominantly twofold: i) from digital elevation models (DEMs) or ii) direct measurements of water level elevation with respect to the riverbed (Table 3). Channel bed slope (Ganti et al., 2014) and channel-floodplain slope (Brooke et al., 2022) are rarely used, and several publications do not specify their data source (Table 3). Slope can be obtained from a single location or section of the river path, which will result in different slope estimates depending on the chosen location (see *4.1 Location to measure slope and depth*). DEMs based on satellite imagery are used to generate elevation profiles along centerlines of river paths so the slope of the river water level can be measured (e.g. Hartley et al., 2016). When using direct measurements of river water level to obtain slope, temporal changes may influence the slope estimates. Discharge variations and tidal fluctuations cause differences in water levels, albeit that this occurs predominantly in the area of non-uniform flow, which is the backwater zone itself. Nittrouer et al. (2011) take such differences into account by averaging elevation data over an 8-year period.

Several publications list slope estimates for the same rivers (Table 1, Supplemental Table S2) and may differ a factor 2. These differences based on digital elevation models for the same river may result from measuring slope over different sections of the river path (see *4.1 Location to measure slope and depth*). We estimated slope over the exact same river segment based on gauging data and DEM for the Mississippi river, which results in 8.5 x 10^{-5} and 6.75 x 10^{-5}, resulting in backwater length estimates of

365 km and 459 km, respectively (Fig. 3F, Supplemental Table S3E). As this segment is in the normal flow reach, differences cannot be ascribed to discharge variations as water surface slopes at different discharges are subequal to each other (Nittrouer et al., 2011). The cause of this difference is currently elusive.

Recommendations: The disadvantage of slope estimates with DEMs is that satellite imagery provides static snapshots. It is difficult to assess whether the river water level in the river contained in the model represents low, normal or high river stages, or perhaps a mixture as the river path is likely captured during multiple satellite orbits. Additionally, coastal dynamics, such as daily to annual tides and wave conditions might impact the distal reaches of the elevation profile. However, a huge advantage of DEMs is that they are available globally, which contrasts with localized and scarcely available data sets with direct measurements of water surface elevation. As with the DEMs, depending on the time of the year, differences in discharge may affect steepness of the water elevation profile, but this will be mostly prominent in the area of non-uniform flow, i.e. the backwater zone, and can be overcome by averaging elevation data over a several year period. We consider both methods (slope estimates obtained DEMs and direct measurements of water level or riverbed elevation) equally recommendable for obtaining backwater length estimates in modern river systems.

5. Proposed workflows, error sources and uncertainty ranges to estimate backwater length

For both ancient and modern river systems, we propose separate workflows to obtain the input parameters (channel depth and slope) necessary to estimate backwater length. These workflows (i.e. A1–A4 for ancient settings, M1–M7 for modern settings) aim to minimize ambiguity in resultant backwater length estimates and are tailored to differences in available data to maximize practicality and reproducibility. Additionally, we list uncertainties involved in each workflow, which result from inherent scatter in previously established relationships.

5.1. Ancient settings – workflows to obtain backwater length

Four different workflows are proposed to estimate backwater lengths in ancient strata (workflow A1–A4, Fig. 4), based on different input data for obtaining bankfull thalweg channel depth and slope and subsequent differences in uncertainty ranges (Fig. 5).

Workflow A1 and A2 combine grain size data to estimate slope with either direct measurements of fully preserved channel story thickness as a proxy for bankfull thalweg channel depth (workflow A1) or determine bankfull thalweg channel depth based on average cross-set thickness (workflow A2) (Fig. 4). Bankfull thalweg channel depth (d_{bf}) (i.e. workflow A1) can be estimated from story thickness (step A, Fig. 4) but an appropriate compaction factor needs to be applied (step B, Fig. 4) (Long, 2021). Note that true thalweg depth should be measured from completely preserved single-story trunk channel deposits and apparent thickness estimates stemming from outcrops affected by tectonic tilt should be corrected to true thickness. Workflow A2 determines bankfull thalweg channel depth based on average cross-set thickness (steps B, C, and D, Fig. 4). In case maximum cross-set height is collected in the field, this should be converted to mean cross-set thickness using $h_{xs\text{-}mean} = 0.7(\pm 0.01)h_{xs\text{-}max}$ (Lyster et al. 2021) before being decompacted (step B). Cross-set thicknesses should be measured on trough and/or planar cross-bedding, as these bedforms are indicative of bedload transport. The next step (step C) is to establish mean dune height using equation 2 from which bankfull thalweg channel depth (i.e. formative flow depth) can be calculated using equation 3 (step D). Slope is estimated using average grainsize (D50) and average bankfull channel depth for both workflow A1 and A2, using equation 4 (steps E and F, Fig. 4). Key is to perform grainsize analysis on a representative sample for bedload transport at times of formative (bankfull) discharge, which is typically the lowest bedform above the basal channel lag (c.f., Holbrook & Wanas, 2014).

Workflow A3 and A4 derive an estimate of slope based on bankfull channel width (w_{bf}) instead of grain size (workflow A1 and A2, Fig. 4) and combine this with previously listed ways to obtain bankfull thalweg channel depth based on fully preserved channel story thickness (steps A and B, workflow A1 and A3, Fig. 4) or empirically based on average cross-set thickness (steps B, C and D, workflow A2 and A4, Fig. 4). Slope is estimated from bankfull channel width (w_{bf}) by using equation 6 (steps G and H, Fig. 4). Channel widths should be corrected for channel elements from outcropping bodies cut at an angle to cross-stream direction. Alternatively, bankfull width can be estimated from bankfull thalweg channel depth using $w_{bf} = 16.872\ d_{bf}^{1.169}$ (Long, 2021). If sinuosity (P) is known, we recommend to use $w_{bf} = 16.293\ d_{bf}^{1.198}$ for low sinuosity rivers (P<1.3), $w_{bf} = 17.338\ d_{bf}^{1.168}$ for intermediate (1.3<P>1.7), and $w_{bf} = 17.458\ d_{bf}^{1.230}$ for high sinuosity systems (P>1,7) (Long, 2021).

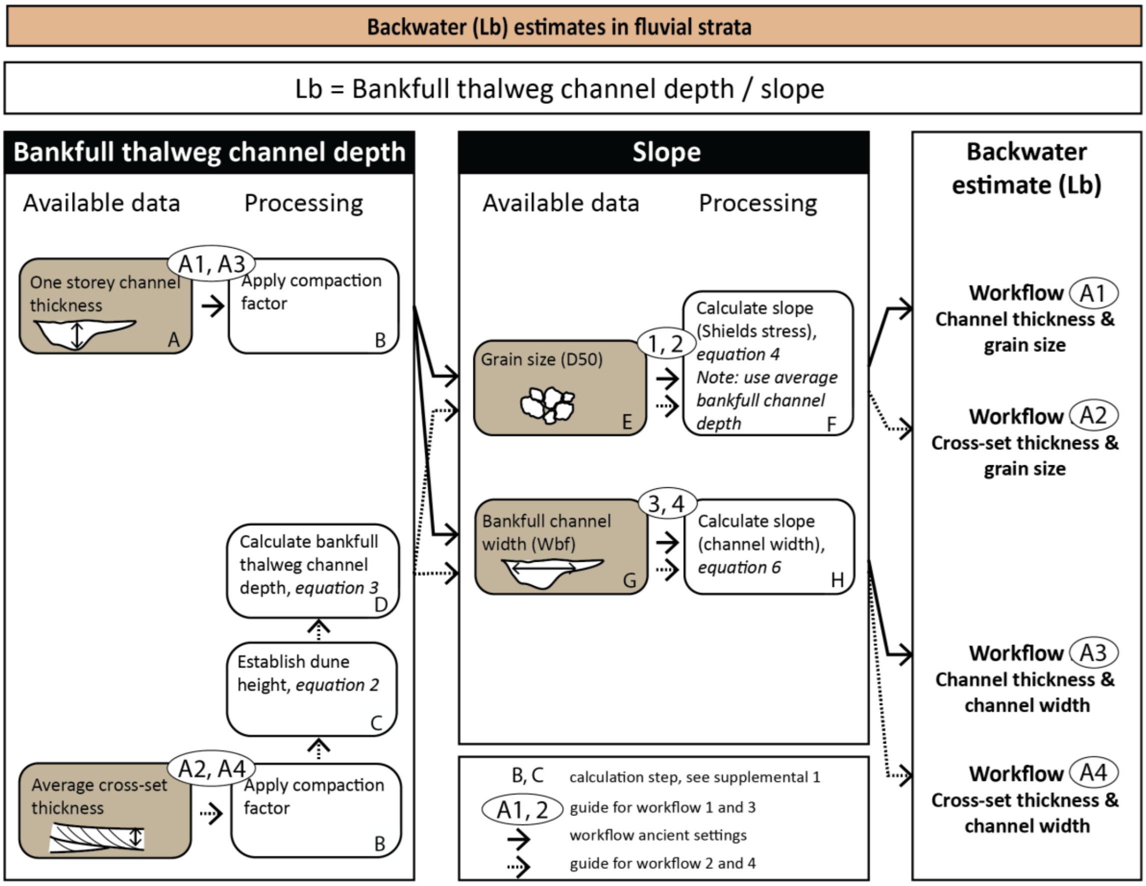

Fig. 4. Workflow recommendation for estimating backwater length (Lb) in ancient settings (A1–A4), based on different input data (brown boxes) to obtain bankfull thalweg channel depth and slope. Workflow numbers are annotated as well as data collection and/or calculation steps (A-H white boxes) that need to be executed (e.g. workflow A1 is based on step A, B, E, and F) (see also Fig. 5 and Supplemental text S2 and S3). Note that step F uses mean bankfull flow depth, and not bankfull thalweg flow depth. Therefore, if a proxy used for channel depth represents bankfull thalweg depth (e.g. fully preserved channel story thickness measured on an outcrop) a

conversion to mean bankfull flow depth will need to be made before inserting this channel depth in the equation (see equation 7 in section 4.3. Channel depth type).

5.2. Ancient settings – error sources and uncertainty ranges

We utilize cumulative uncertainty estimates for eventual prioritization of workflow recommendation (see *6.2 Workflow recommendation*). Each step within the workflows has an uncertainty range, due to natural scatter in previously established relationships and uncertainties in observation and collection of (field) data parameters. Propagation of these uncertainties affect the cumulative uncertainty in the backwater length estimate (Fig. 5).

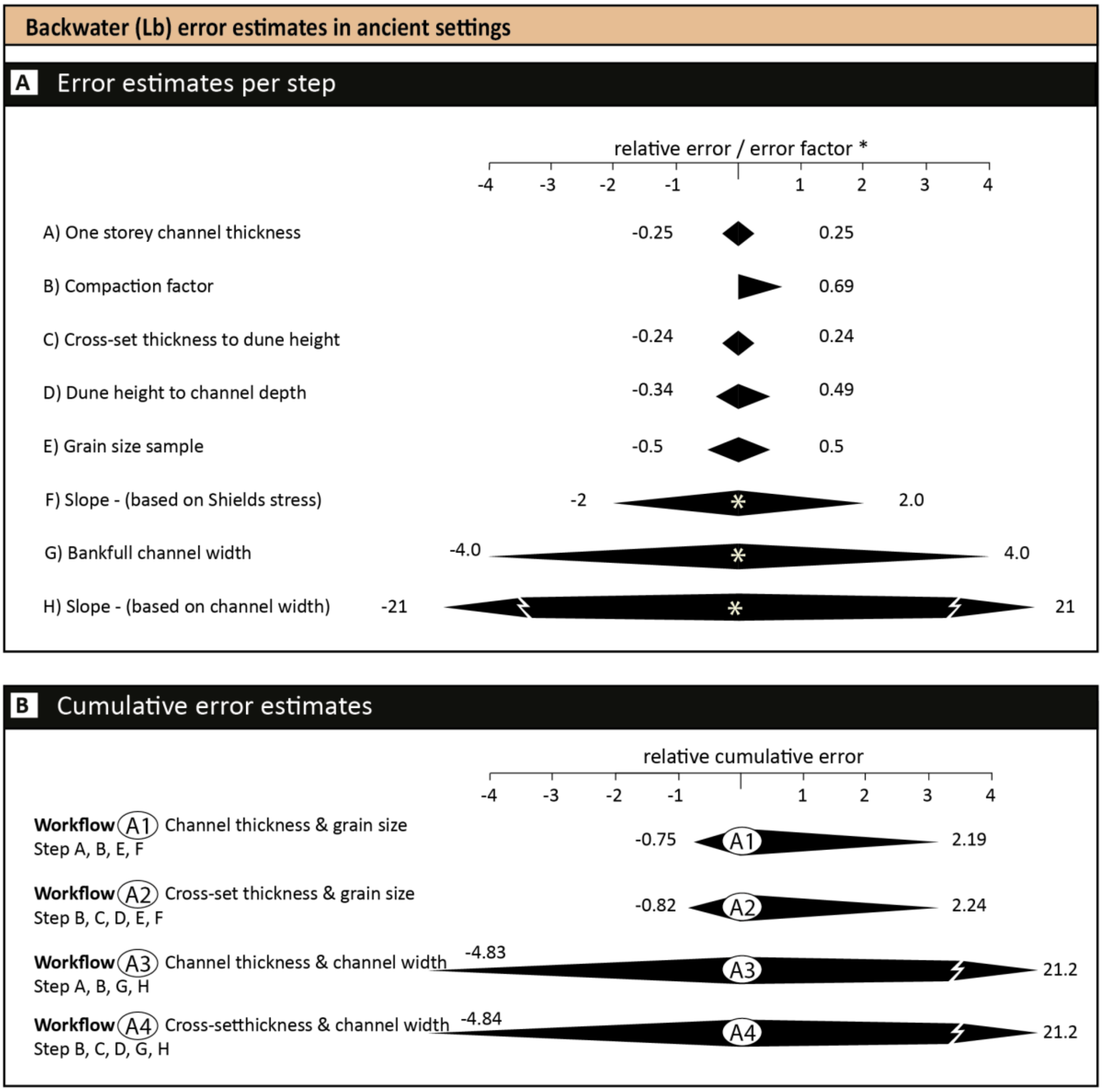

Fig. 5. Display of error magnitudes. (A) Estimated errors for each step or calculation used in the recommended workflows. Letters A-H related to steps used in Fig. 4. These errors represent current estimates that approximate the maximum generalized error of each step, and reflect a 50% (step D) or 95% (all other steps) confidence interval resulting from inherent scatter in previously established relationships or potential errors during data collection. The difference between errors is annotated in relative error and uncertainty factors. See Supplemental text S1 and S2 for more details. (B) Cumulative error estimates for each workflow calculated by using an error propagation equation based on taking partial derivatives with respect to the variable with the uncertainty. See Supplemental text S3 for calculation details and text (sections 2 and 4) for further discussion and references. By example, a backwater length estimate of 100 km obtained by applying workflow 1, has a minimum of 25 km (i.e. 100 km – (0.75 x 100)) and a maximum of 319 km (i.e. 100 km + (2.19 x 100)) when taking its uncertainty ranges into account.

Obtaining channel story thickness (step A, used in workflow A1 and A3. Fig. 4) is considered to have a 25% error, based on potential for misidentification of complete channel-fill story thickness (Holbrook & Wanas, 2014). A 25% error translates to a minimum and maximum relative error of ± 0.25 (Fig. 5, Supplemental text S1, S2). Application of a compaction factor (step B, used in workflow A1 and A3. Fig. 4) should ideally be estimated based on thin-section data. If not available, a compaction factor of 1.1 is commonly used (Holbrook & Wanas, 2014; Long, 2021), but it is important to acknowledge that common range is between 1.0 and 1.69 (Long, 2021). This results in a relative error of 0 to 0.69 (Fig. 5, Supplemental text S1, S2). Establishing mean dune height from mean cross set thickness (step C, Fig. 3) is done based on an empirical relationship, equation 2 (Leclair & Bridge, 2001), and involves a minimum and maximum relative error of ± 0.24 (Fig. 5, Supplemental text S1, S2). Establishing bankfull thalweg channel depth from mean dune height (step D, Fig. 3) is done based on an empirical relationship, equation 3 (Bradley & Venditti, 2017), and involves a minimum and maximum relative error of +0.49 and –0.34 (Fig. 5, Supplemental text S1, S2).

Obtaining slope can be based on grain size and its empirical relation with Shields stress (steps E and F, workflows A1 and A2,Fig. 4) or derived from bankfull channel width (step G and H, workflow A3 and

A4, Fig. 4). Selecting a representative grain size sample (step E) is considered to have a 50% error, based on common challenges when identifying representative bedload samples in outcrop and core data (Holbrook & Wanas, 2014). A 50% error translates to a minimum and maximum relative error of ± 0.50 (Fig. 5). Calculating slope based on Shields stress using equation 4 (step F, Fig. 4) is considered to have an uncertainty factor of ± 2, which is related to uncertainty in the bankfull Shields number (Holbrook & Wanas, 2014) (Fig. 5). We assume that channel slope is in equilibrium with the bed shear stress required to move bedload. Measuring bankfull channel width (step G, Fig. 4) is prone to an uncertainty factor of ± 4 when estimated based on empirical relationships (Hajek & Wolinsky, 2012; Blum et al., 2013; Holbrook & Wanas, 2014) in case of core data (Fig. 5). In outcrops, uncertainty arises from outcropping channel bodies cut at an angle to the reconstructed cross-stream direction. Calculating slope based on its empirical relation with bankfull channel width using equation 6 (step H, Fig. 4) involves a uncertainty factor of 21 (Fig. 5, Supplemental text S1, S2).

Combining all uncertainties involved in the execution of a workflow provides cumulative errors, which are calculated by:

$$\frac{\Delta Q}{|Q|} = \sqrt{\left(\frac{\Delta a}{\mathrm{a}}\right)^2 + \left(\frac{\Delta \mathrm{b}}{\mathrm{b}}\right)^2 + \cdots + \left(\frac{\Delta z}{\mathrm{z}}\right)^2} \qquad (10)$$

with ΔQ/|Q| being the cumulative relative error and Δa/a, Δb/b, etc. being the relative error of individual steps in the workflows (see Supplemental text S3).

Cumulative relative errors range between 2.19 (workflow A1 and A2) and 21.2 (workflow A3 and A4) when following the proposed workflows for estimating backwater lengths in ancient settings (Fig. 5). The largest proportion of these uncertainty ranges results from errors in slope estimates.

5.3. Modern settings – workflows to obtain backwater length

Seven different workflows are proposed to estimate backwater lengths in modern river systems (M1–M7), based on different types of input data for bankfull thalweg depth and two methods to measure slope (Fig. 6). We distinguish between the use of the intersection method in which the distance between the river mouth and the location where riverbed elevation intersects sea level provides the backwater length (Nittrouer et al., 2011; Blum et al., 2013; Fernandes et al., 2016; Gugliotta et al., 2017; Smith et al., 2020) and the indirect estimate of backwater length (L_b) by calculating $L_b = h/S$, with h is bankfull thalweg channel depth and S is slope (Hartley et al., 2016; Ganti et al., 2016; Brooke et al., 2020, 2022; Prasojo et al., 2022). Among the studied publications for this review, a match between changes in flow conditions and intersection of the river bed with sea level has been demonstrated in the Mississippi River and Trinity river (Nittrouer et al., 2011; Smith et al., 2020).

The intersection method implies that either the absolute height of the riverbed profile is measured directly with a hydrographic riverbed survey (workflow M1), or the channel depth is subtracted from the river water level elevation (workflows M2 and M3) (Figs. 6 and 7). The intersection method requires that bankfull thalweg channel depth and river slope are estimated over long distances. Workflow M1 uses the absolute height of the riverbed profile obtained with a hydrographic riverbed survey. The backwater length is where the riverbed profile intersects sea level and no slope profile is needed. In workflow M2, channel depth is measured directly with a bathymetric survey. As the conditions will likely not reflect bankfull conditions, the obtained channel depth needs to be converted to bankfull, for which we recommend to use equation 7. Workflow M3 allows for a desktop-approach; channel width obtained from satellite imagery over a long segment of the river profile can be used to obtain bankfull thalweg channel depth, using equation 8. To find the intersection location of the riverbed with sea level, bankfull thalweg channel depth profiles obtained with workflows M2 and M3 should be combined with slope profiles obtained from water elevation profiles (e.g. from gauge data) or digital elevation models (Figs. 6 and 7).

Backwater length estimates based on $L_b = h/S$ (i.e. workflows M4–M7*)* require bankfull thalweg channel depth (h) and slope (S) ideally obtained from the normal flow reach. However, data needed to assess the position of the normal flow reach (i.e. water level elevation data at both normal and high discharge stages to assess sub-equality of their slope profiles; subequal profiles reflect uniform flow conditions) is not always available. For pragmatism, we suggest to collect input parameters at least updip of the apex (depth from one location, slope over long distances), as there is a presumed match between the location of the apex, backwater length and hence transition into normal flow conditions (Chatanantavet et al. 2012; Chadwick et al. 2019), albeit that rivers with backwater zones extending beyond the apex are common (Hartley et al. 2016).

Workflow M4 uses channel width obtained from satellite imagery from a location updip from the apex (or from the normal flow reach, if known) which can empirically be converted into bankfull thalweg channel thalweg depth, using equation 8 (Fig. 6). Workflow M5 obtains bankfull thalweg channel depth from a cross-sectional profile from a location updip from the apex (or from the normal flow reach, if known) (Fig. 6). Workflow M6 estimates bankfull channel thalweg depth based on empirical relationships with discharge and bed friction coefficient using equation 9 (Fig. 6). Finally, workflow M7 uses channel bed grain size data as an input parameter to utilize empirical relationships based on Shields stress, using equation 4 (Fig. 6). The grain size sampled should be collected from a location updip from the apex or from the normal flow reach if known. Note that the resulting channel depth represents *mean* channel depth and needs to be converted to bankfull thalweg channel depth using equation 7 (Fig. 6, Supplemental table 4). Slope should be collected over long distances for workflows M4–M7, preferably in the normal flow reach or otherwise updip of the apex, by using digital elevation models or based on water elevation profiles obtained from direct measurements (A and B in Fig. 6). Combining bankfull thalweg channel depth and slope will provide backwater length estimates.

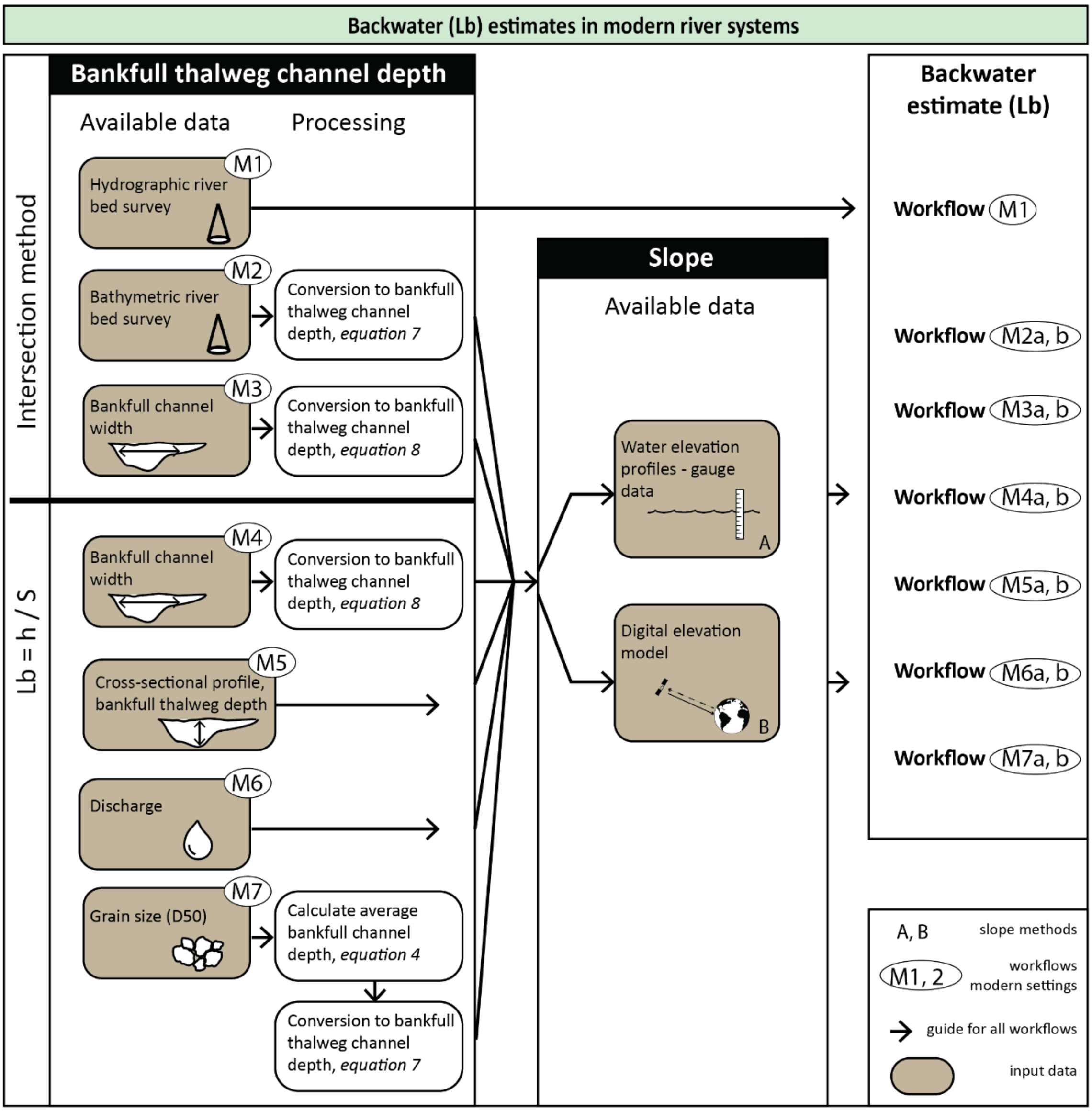

Fig. 6. Workflow recommendation for estimating backwater length (Lb) in modern river systems (M1–M7), based on different input data (brown boxes) to execute the intersection method or obtain bankfull thalweg channel depth and slope.

Fig. 7. Intersection method (workflows M2 and M3). Bankfull thalweg channel depth measurements are obtained along the river profile. These depth estimates can be obtained with direct bathymetric measurements (workflow M2), or empirical relationships with channel width (workflow M3). These depths are subtracted from the river (i.e. water level) elevation profile. The backwater length is the distance between the river mouth and the location where the riverbed elevation intersects sea level.

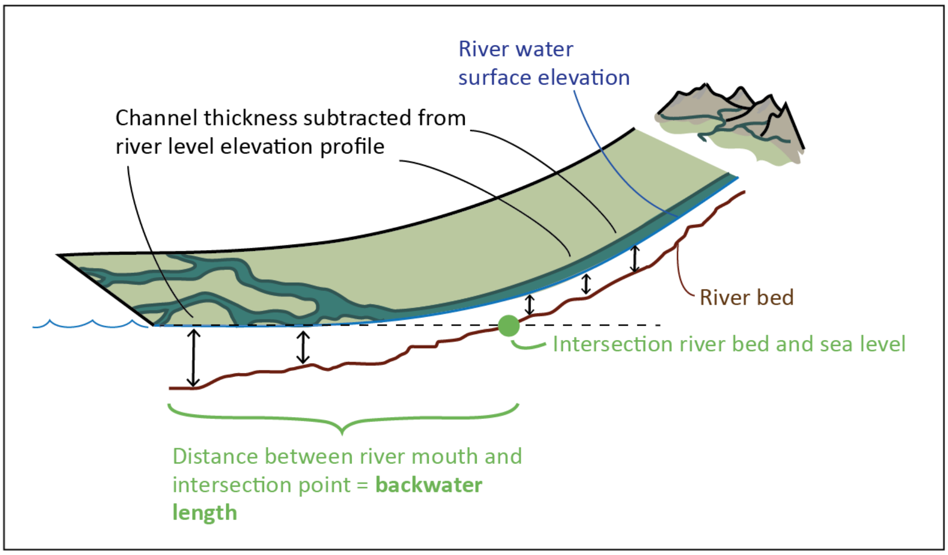

5.4 Modern settings – error sources and uncertainties

Assessment of cumulative uncertainty ranges for each workflow forms the base to prioritize workflow recommendations. However, most previously proposed workflows include one or several aspects or equations with unquantified uncertainty ranges or are based on data sets inaccessible for statistical analysis. As quantification of these is beyond the scope of this paper, we only briefly list these uncertainties below.

Workflow M1 involves the performance of a hydrographic survey resulting in absolute heights of the riverbed (Fig. 6). This workflow has minimal uncertainties, as the data is directly collected in the field and no data manipulation is needed to find the intersection with sea level. Workflow M2 is based on executing of a bathymetric survey to find channel depth along the river profile (Fig. 6). It assumes data collection at times of mean flow conditions and therefore involves conversion to bankfull thalweg channel depth. This conversion is empirical and is inherently prone to uncertainty ranges, albeit that the r^2 value of this relation is remarkably high ($r^2 = 0.93$; Long et al. 2021). Workflows M3 and M4 utilize a channel width to depth ratio (Fig. 6). Such ratios should generally be considered approximate as they typically change in relation to channel style, sinuosity, system scale, tide-influence, climate, etc. (references in Long et al. 2021). Workflow M5 obtains bankfull thalweg depth from a cross-sectional profile, which will provide an accurate bankfull thalweg depth for that particular location (Fig. 6).

Workflow M6 uses the empirical relationship based on the characteristic water discharge, a bed friction coefficient, slope and channel width to estimate bankfull channel thalweg depth (Fig. 6) (Parker et al., 2007). Characteristic discharge is often calculated by taking the peak annual flood event with a two-year recurrence interval. In other cases, monthly discharge is converted to daily discharge using empirical transformations for different climates (Beck et al.,2018) which has an inherent scatter in its relationship. Additionally, selection of the bed friction coefficient and estimating slope and channel width will bear uncertainties as well. Altogether, this suggests that the resulting channel depth is rather approximate. Workflow M7 uses average grain size (D50) as input parameter to an empirical relationship with Shields dimensionless shear stress, slope, average bankfull channel depth and submerged dimensionless density. This involves uncertainty in collecting a sample representative for bedload transport and estimating a characteristic slope and channel depth.

In general, we consider the intersection method (workflows M1–M3) more accurate than the indirect approach (i.e. Lb = h/S, workflows M4–M7) because of the abovementioned uncertainties in M4–M7, in addition to that the latter typically involves channel depth information obtained from only one location, contrasting data collecting over long distances (i.e. the intersection method) which thereby smoothens the generally irregular riverbed profile.

6. Discussion

6.1. Testing the applicability and geological meaning of backwater estimate ranges

6.1.1. Rock record case study – Dakota Group, USA

To test the previously proposed workflows to obtain backwater estimates in ancient settings, we utilize the Cenomanian Mesa Rica Sandstone (Dakota Group, USA) which represents contemporaneous fluvio-deltaic deposition in the Western Interior Basin and is exposed along a down-depositional dip 400 km transect in southeast Colorado and northeast New Mexico (e.g. Holbrook, 1996; Scott et al., 2004; Oboh-Ikuenobe et al., 2008; Van Yperen, Holbrook, et al., 2019; van Yperen et al., 2021). Previous studies on Mesa Rica Sandstone channel deposits provide all the input parameters needed; grainsize data, average channel depth and width and average cross-set thickness collected in normal-flow reaches (Van Yperen et al., 2021; Fig. 8, Supplemental Table S4).

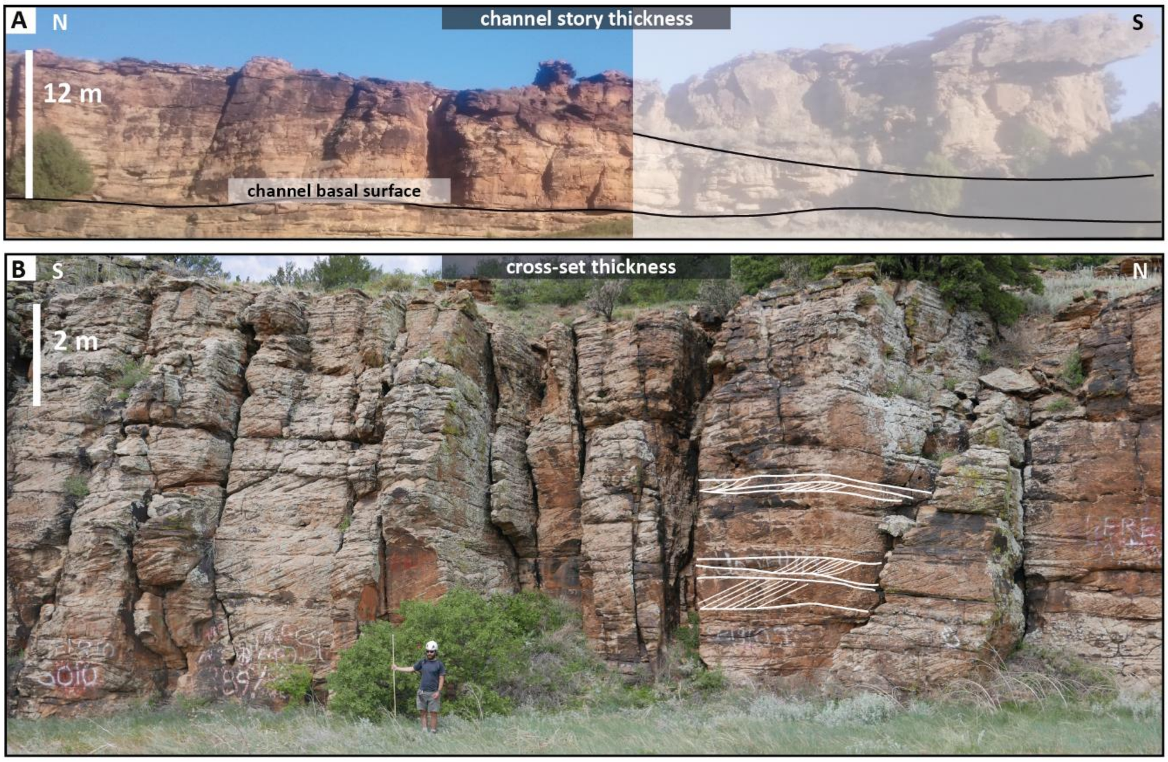

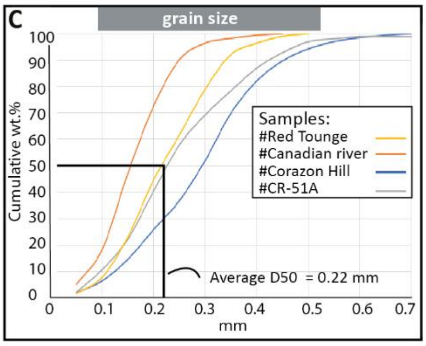

D

Input data			Output - Lb (km) Lb (km)*	Output - Lb (km) Lb (km)**	Output - Lb dimensionless r/Lb♦	Output - Lb dimensionless r/Lb♦♦
Workflow A1 (channel storey & grain size)		mean	188	188	1.0	1.0
input data channel thickness:	13.2	max	599	326	3.2	1.7
input data slope:	7.02E-05	min	47	141	0.3	0.8
Workflow A2 (crossbed thickness & grain size)		mean	117	117	0.6	0.6
input data crossbed thickness:	9.2	max	380	220	2.0	1.2
input data slope:	8.94E-05	min	116	68	0.6	0.4
Workflow A3 (channel storey & channel width)		mean	23	23	0.1	0.1
input data channel thickness:	13.2	max	524	41	2.2	0.2
input data slope:	5.64E-04	min	15	18	0.1	0.1
Workflow A4 (crossbed thickness & channel width)		mean	16	16	0.1	0.1
input data crossbed thickness:	9.2	max	365	29	1.6	0.1
input data slope:	5.64E-04	min	8	10	0.0	0.0

Fig. 8. O**utcrop case study**: examples of input parameters obtained from the lower Cretaceous Mesa Rica Sandstone (Van Yperen et al., 2021) used to estimate backwater length following all four proposed workflows (A1–A4). (A) Single-story channel depth are on average 12 m thick in the Mesa Rica Sandstone depositional system, Purgatoir Canyon (Colorado). (B) Example of cross-stratification bedsets in the Mesa Rica Sandstone, Mosquero (New Mexico). (C) Particle size distribution curves for four grain size samples from the lowermost bedforms from trunk channels. The average D50 based on these four samples is 0.22 mm. (D) Table listing input parameters used to apply all four workflows to estimate backwater length. See Supplemental text S3 and S4 for details of each parameter taking into account error propagation based on uncertainty ranges resulting from

inherent scatter in previously established relationships. Lb = backwater length, * and ** = including propagated errors in obtaining both channel depth and slope, and only channel depth, respectively, r/Lb ♦ and r/Lb ♦♦ = non-dimensionelized backwater length (Lb) with respect to workflow A1 (Lb = 152 km) by multiplication of propagated errors of both channel depth and slope, and only channel depth, respectively. The green box highlights non-dimensionlized distances depicted on Fig. 9.

The application of workflows A1–A4 (Fig. 4) based on these parameters shows that workflows A1 and A2 result in different backwater length estimates (i.e. mean Lb estimates of 188 km and 117 km for workflows 1 and 2, respectively), whereas workflows A3 and A4 have significant lower mean Lb estimates (i.e. mean Lb estimates of 23 km and 16 km, respectively) (Fig. 8, Table S4). The low values of workflows A3 and A4 are mainly due to slope estimates inferred from bankfull channel width (workflows A3 and A4) being one factor steeper than slope estimates based on grainsize (workflows A1 and A2). Workflow A2 results in a significantly shorter backwater length than workflow A1 because of a shallower bankfull thalweg channel depth and a slightly steeper slope.

We calculated maximum Lb estimates in two ways: i) by multiplication of propagated errors of both channel depth and slope (Lb* in Fig. 8, Table S4), and ii) by multiplication of propagated errors in only channel depth (Lb** in Fig. 8, Table S4). The first approach results in maximum Lb estimates of 599 km and 380 km for workflows A1 and A2, respectively, whereas the second approach results in maximum Lb estimates of 326 km and 220 km for workflows A1 and A2, respectively.

Characteristics of fluvial channel-fill deposits along the down-depositional dip transect of the Mesa Rica Sandstone allow for comparison with backwater lengths resulting from the derived estimates (Fig. 8, Table S4). This suggests the following: i) changes in fluvial architectural style linked to backwater conditions in the Mesa Rica Sandstone depositional system indicate a backwater length of ~180 km (Van Yperen et al., 2021), which relates well to *mean* estimate resulting from workflow A1, but mean estimates following workflows A2, A3 and A4 are far off. ii) *Maximum* backwater lengths resulting from uncertainty ranges in both channel depth and slope (i.e. Lb*) for workflows A1 and A2 (Lb* is 599 km and 380 km, respectively) (Fig. 8D, Table S4) occur in an area along the depositional profile where multivalley channel deposits dominate the fluvial architectural style. These represent buffer valleys (*sensu* Holbrook et al., 2006) and their infill characteristics area controlled by temporal fluctuations in upstream sediment and water discharge (Holbrook, 2001). Their scour depth profile is tens of meters (i.e. several channel-thicknesses) above sea level, which is evidently outside backwater influences. Excluding the uncertainty ranges related to slope errors (i.e. Lb**) lowers the uncertainty and hence, maximum values for backwater length estimates are closer to the mean values as when uncertainties for both channel depth and slope are taken into account (i.e. Lb*). The maximum backwater for workflow A1 (i.e. 326 km, Lb**, Fig. 8D, Table S4) occurs in an area dominated by multivalley deposits, whereas the maximum for workflow A2 (i.e. 220 km, Lb**) is close to the mean of workflow A1 (i.e. 188 km) and relates to a change in fluvial architectural style from a mix of single-story trunk channel deposits and multivalleys, to sheet forming single-.story channel deposits.

A narrow 'updip backwater transition zone' is the result of this case study based on the results of workflows A1 and A2 (Fig. 9). In this zone, there is an overlap of the derived backwater length estimates and their uncertainty ranges, which matches the occurrence of reported changes in channel architectural style. The lower and upper limit of this zone are defined by the lower limit of the backwater length estimate of workflow A1, and upper limit of the backwater length of workflow A2. This illustrates the significant different backwater lengths resulting from these workflows. However, this case study also shows that the mean backwater length of workflow A1 and maximum backwater length of workflow A2 plot in proximity to the outcrop-based backwater length estimate based on changes in fluvial architectural style. Maximum ranges of backwater lengths are most trustworthy when excluding errors in slope estimates.

We argue that the dimensionless updip backwater transition zone represents the most reliable estimate of the updip limit of the backwater zone and is potentially applicable to other systems as well. However, to further define and test this dimensionless updip backwater transition zone, more outcrop studies are needed in which all workflows are calculated and compared with changes in fluvial architectural style.

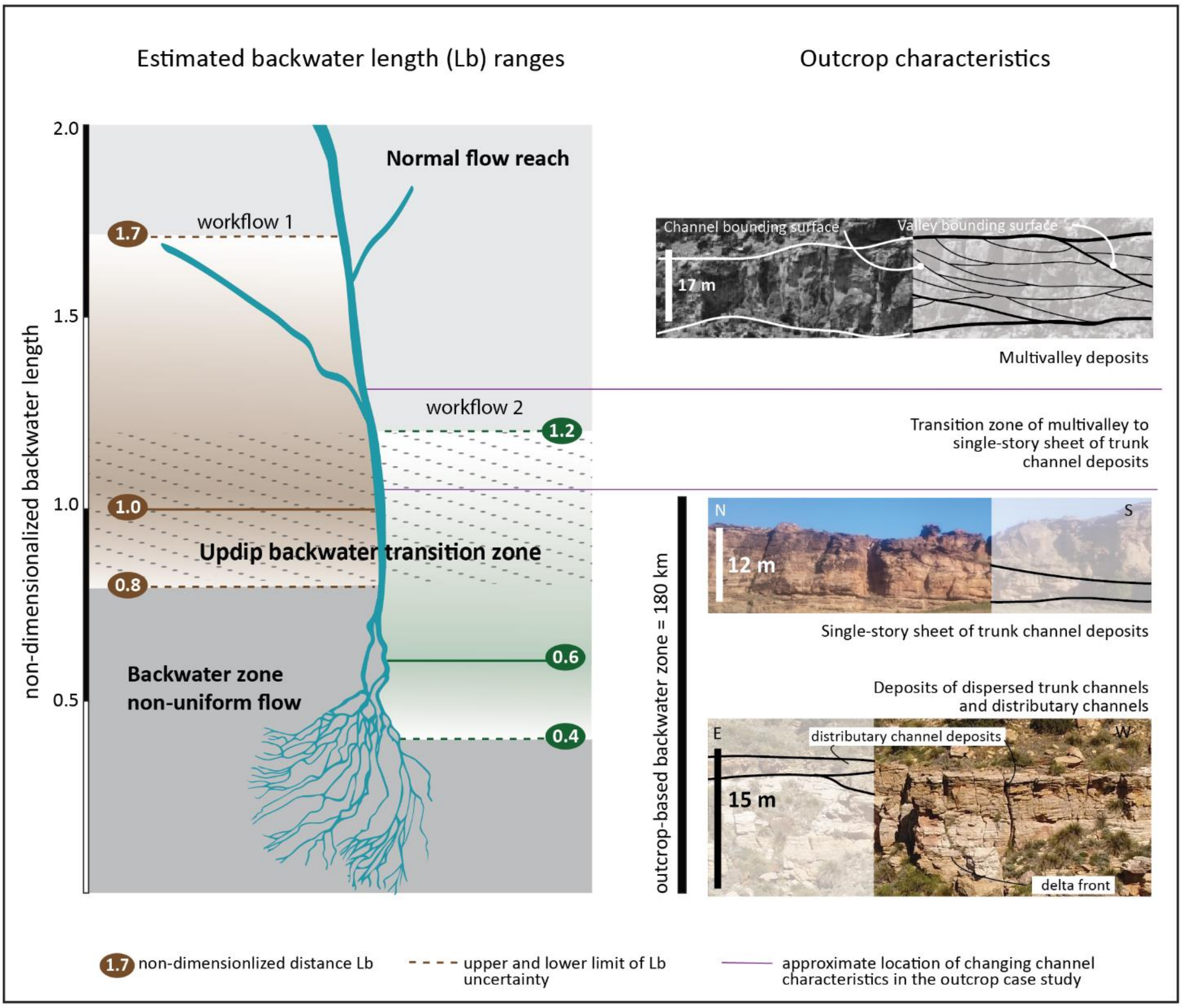

Fig. 9. **Dimensionless backwater length estimates** resulting from workflow A1 (in brown) and A2 (in green) projected onto a schematic representation of the ancient fluvio-deltaic depositional system selected as case study (Cretaceous Mesa Rica Sandstone, USA). Lower, mean and upper values of backwater length estimates are non-dimensionlized with respect to the mean backwater length from workflow A1 (i.e. 188 km). The overlapping (shaded) area represents the dimensionless updip backwater transition zone, where results from the two workflows overlap and hence represents the most reliable estimate of the updip limit of the backwater zone. Outcrop characteristics representing a summary of the main fluvial architectural styles present in the case study are relevant to assess whether there is an actual link between backwater estimates and observable changes in fluvial architecture. Outcrop pictures modified from Holbrook (2001), van Yperen et al. (2021).

6.1.2. Modern case study - Mississippi River

To test the proposed workflows (M1–M7) to obtain backwater estimates in modern river systems, we selected the Mississippi river (USA) based on availability of a continuous channel bed profile and water elevation profiles at different discharge stages in its lower 1050 river km (Nittrouer et al., 2011). Additional input parameters such as discharge (Prasojo et al., 2022), grainsize and cross-sectional profiles (Nittrouer et al., 2012) and bankfull channel width are available or can be easily obtained from satellite imagery. Only workflow M2 cannot be tested as bathymetric survey data along the lower Mississippi river is not readily available.

Application of workflow M1 provides the most direct identification of intersection between thalweg channel depth and sea level, which occurs around 680 river km above Head of Passes and matches changes in flow conditions (Fig. 10A, B). The river bed profile based on width:depth ratios (workflow M3) intersects with sea level around 800 km (Fig. 10A, B, Supplemental Table S5, S6). Workflows M4–M7 obtain backwater length estimates indirectly (i.e. Lb = h/S) and use slope collected in the normal reach area (i.e. 650 – 1050 km) based on water elevation profiles obtained from both DEM and bankfull discharge stage. These should theoretically provide the same slope as water surface slopes are uniform and independent of water discharge in the normal flow reach (Nittrouer et al., 2011, 2012), but the DEM provides steeper slopes hence resulting in shorter backwater lengths. Workflows M4–M7 all results in backwater length distances (i.e. between 163 – 491 river km) shorter than the actual 680 river km at which the riverbed intersects sea level (Fig. 10A-C, Table S5). Backwater length estimates based on bankfull thalweg channel depth derived from discharge and grain size (Workflows M6 and M7, respectively) plot in the non-uniform flow zone whereas the results based on bankfull thalweg channel depth derived from width:depth ratio and cross-sectional profile (Workflows M4 and M5, respectively) plot in the backwater transition zone (Fig. 10B, C). Previously published backwater length estimates based on h/S show a similar range (i.e. between 281 and 480 km, see Table 1).

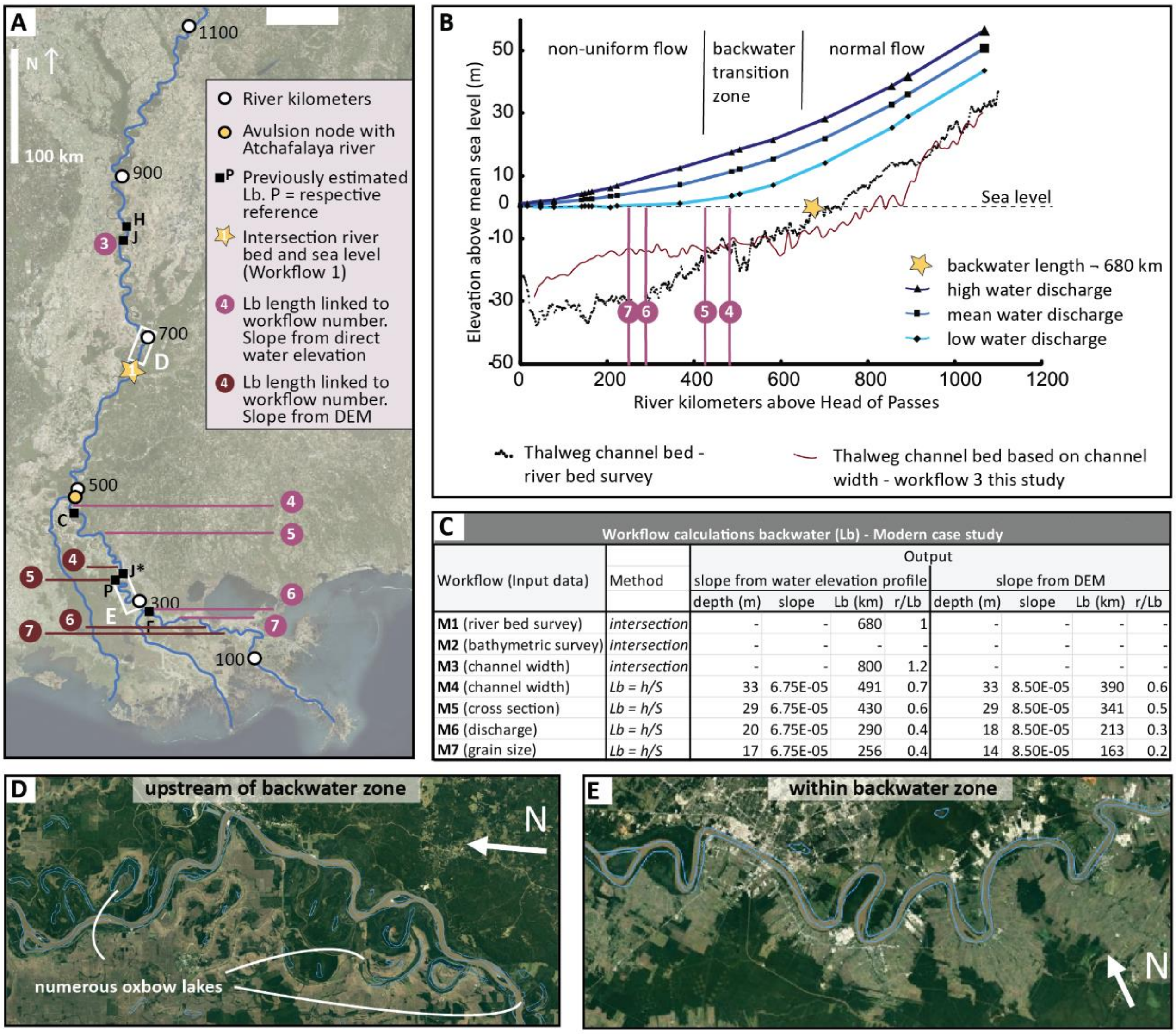

Workflow (Input data)	Method	Output							
		slope from water elevation profile				slope from DEM			
		depth (m)	slope	Lb (km)	r/Lb	depth (m)	slope	Lb (km)	r/Lb
M1 (river bed survey)	*intersection*	-	-	680	1	-	-	-	-
M2 (bathymetric survey)	*intersection*	-	-	-	-	-	-	-	-
M3 (channel width)	*intersection*	-	-	800	1.2	-	-	-	-
M4 (channel width)	*Lb = h/S*	33	6.75E-05	491	0.7	33	8.50E-05	390	0.6
M5 (cross section)	*Lb = h/S*	29	6.75E-05	430	0.6	29	8.50E-05	341	0.5
M6 (discharge)	*Lb = h/S*	20	6.75E-05	290	0.4	18	8.50E-05	213	0.3
M7 (grain size)	*Lb = h/S*	17	6.75E-05	256	0.4	14	8.50E-05	163	0.2

Fig. 10. Case study on the Mississippi river: (A) Lower 1100 river km of the Mississippi River with previously published estimations of the landward extend of backwater length, and all seven workflows proposed in this study (M1–M7). ■ previously published backwater lengths: J = Table 1 in Jerolmack (2009), J* = Fig. 14 in Jerolmack (2009), C = Chatanatavet et al. (2012); F = Fernandes et al. (2016); H = Hartley et al. (2016), P = Prasojo et al. (2020). (B) The intersection method based on direct measurements of the riverbed (workflow M1) results in a backwater length of 680 km (modified after Nittrouer et al., 2012). Upstream of this, the thalweg channel bed slope and water surface slopes at different discharges are subequal to each other which is characteristic for normal flow reach. An updip backwater transition zone occurs between ~400 and ~700 river km (Nittrouer et al., 2012). Backwater lengths resulting from workflows M4-7 are projected onto the profile. (C) Input data, method, and resulting bankfull channel depth for each workflow. Workflow M2 was not executed as not bathymetric

survey data is available. Note that workflows M4-7 are performed twice, with slope derived in the normal flow reach from the bankfull water elevation profile from gauging data (Nittrouer et al., 2011) and Digital Elevation Model (DEM). See Supplemental Table 4 for additional details. (D) and (E) illustrate a decrease in meander migration rates and channel-belt width/thickness ratio within the backwater zone. Note the abundance and absence of oxbow lakes close to the upstream limit of the backwater zone (D) and within the backwater zone (E), respectively. A further narrowing of the channel belt just downdip of inset (E) has been assigned to avulsion-driven bifurcation rather than backwater effects (Gugliotta & Saito, 2019).

A mismatch between the riverbed intersection with sea level and flow-type transition (at 680 river km, workflow M1) and derived backwater length estimates (between 163 – 491 river km, workflows M4–M7*,* Fig 10. B, C) can theoretically result from three causes: because the derived backwater length estimates are all shorter than the intersection length, the input parameters are not representative and either i) bankfull thalweg depth is too shallow, or ii) the slope is too steep. Alternatively, because the resulting backwater lengths of M1 versus M4-M7 are significantly different, iii) either the intersection point (M1) or the derived Lb estimates with Lb = h/S (M4-M7) indicates the updip limit of the backwater zone.

Bankfull thalweg depth being too shallow (i.e. reason i) as a possible cause for significantly short backwater length estimates compared to the distance from river mouth to the river bed intersection with sea level, seems unlikely, as we reason that the recommended use of bankfull *thalweg* depth already ensures maximum channel depths. Considering that the used slope estimates might be too steep (i.e. reason ii), using a slope based on the full river profile (from updip to river mouth) instead of retrieved from the normal reach (as used in our case study on the Mississippi river) will provide lower slopes and subsequently longer backwater estimates. Finally, investigation of whether either the intersection point (result of workflow M1) or the derived Lb estimates (results from workflow M4–M7) match the updip limit of the backwater zone (i.e. reason iii) can be based on previously documented changes in sedimentary trends and channel morphology; a) coarsening grain size and channel bed aggradation in the transition zone (~400 – 650 river km) followed by distinct downstream fining (Fig.

11B, Nittrouer et al., 2012), b) increased rates of channel mobility between ~400 – 800 river km (Fig. 11B, Nittrouer et al., 2012), c) progressive decrease of channel-belt width/thickness ratios between ~600 and ~350 km (Fig. 11A, Blum et al., 2013; Fernandes et al., 2016) and d) decreasing meander-bend migration rates between ~800 and ~350 river km (Fig. 11A, Hudson & Kesel, 2000; Fernandes et al., 2016). The latter is illustrated by a change in the abundance of oxbow lakes, for example (Fig. 10 D, E). Contrastingly, analysis of bar deposits reveals no significant changes in bedload-dominated bar deposits and the thickness of heterolithic bar deposits in this reach, but rather rapid decrease and increase, respectively, in the lower 400 river km (Martin et al., 2018). In short, these previously documented changes and their location shows that intersection between riverbed and sea level (at ~680 river km) coincides approximately with the updip extent of the river segment that is characterized by the before mentioned changes, whereas indirectly derived backwater length estimates ($L_b = h/S$) resulting from workflows M4–M7 and previously published values shorter and plot outside or in the lower reaches of the zone of change (Fig. 11C).

It is crucial to incorporate more studies to test and compare backwater length estimates with actual changes in channel morphology and sedimentary trends.

Fig. 11. Documented changes in sedimentary trends and channel morphology and their position along the lower Mississippi river. Green and orange boxes highlight the zones characterized by changes. A) Channel-belt width, channel migration rates and thickness of channel-belt deposits (Fernandes et al., 2016). Average values in black. B) Lateral migration for the lower Mississippi River (Nittrouer et al., 2012). Changes in rates of lateral mobility coincide with the regions changing grainsize (modified after Nittrouer et al., 2013). C) Compilation of previously documented changes in sedimentary trends and channel morphology projected onto the bankfull water elevation profiles and thalweg channel bed profile (modified after Nittrouer et al., 2012). The zone characterized by these changes is depicted as 'zone of change'.

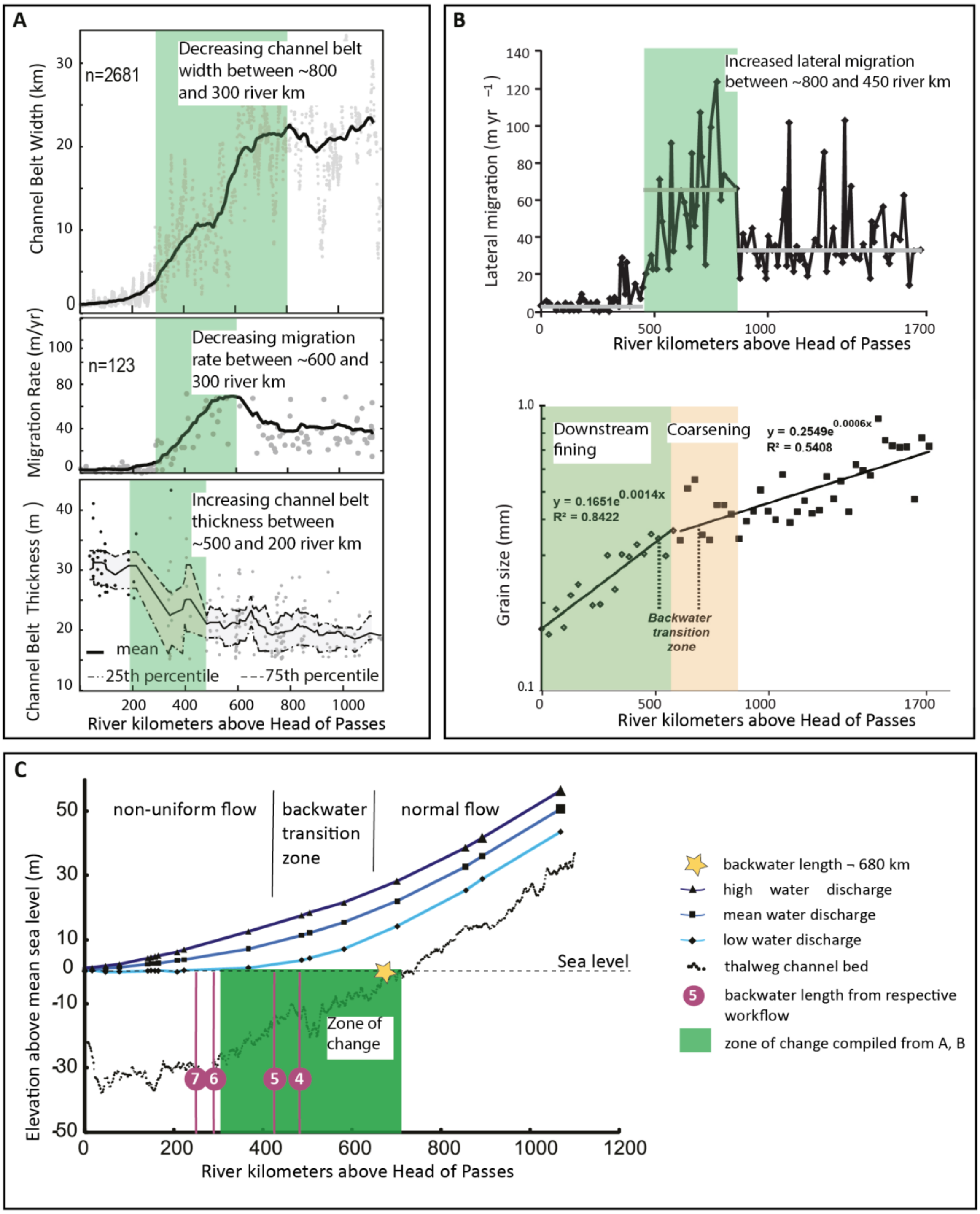
A
Decreasing channel belt width between ~800 and 300 river km
n=2681
Channel Belt Width (km)
Decreasing migration rate between ~600 and 300 river km
n=123
Migration Rate (m/yr)
Increasing channel belt thickness between ~500 and 200 river km
Channel Belt Thickness (m)
mean
25th percentile
75th percentile
River kilometers above Head of Passes
B
Increased lateral migration between ~800 and 450 river km
Lateral migration (m yr −1)
River kilometers above Head of Passes
Downstream fining
Coarsening
y = 0.2549e0.0006x
R² = 0.5408
y = 0.1651e0.0014x
R² = 0.8422
Backwater transition zone
Grain size (mm)
River kilometers above Head of Passes
C
non-uniform flow
backwater transition zone
normal flow
Sea level
Zone of change
Elevation above mean sea level (m)
River kilometers above Head of Passes
backwater length ~ 680 km
high water discharge
mean water discharge
low water discharge
thalweg channel bed
backwater length from respective workflow
zone of change compiled from A, B

957

6.2. Workflow recommendations

6.2.1. Ancient settings

We recommend to consider the mean backwater length of workflow A1 and maximum backwater length of workflow A2 as the most realistic estimates, as they are most closely related to observable outcrop changes in fluvial architectural style (Fig. 9).

In ancient strata, we propose two workflows to obtain backwater length estimates (Fig. 4). Four workflows have been tested, of which workflows A3 and A4 are discarded based on i) the high uncertainty ranges resulting from using channel width as an input parameter to obtain slope and ii) the expected values (i.e. not taking into account the uncertainty ranges) providing backwater lengths that are considered too short to be realistic based on field-evidence from the case study provided in this review (see *5.2 Workflow recommendation*). Workflows A1 and A2 are based on bankfull thalweg channel depth obtained from fully preserved channel story thickness or cross-set thickness, respectively, and both use slope estimates derived from representative grain size samples to be used in empirical relationships based on Shields stress. In case grain size samples are not available, we recommend using the resulting maximum value of workflow A4, as this is closest to the results of workflows A1 and A2 (Fig. 8D).

When input data for both workflows A1 and A2 is available, we recommend to obtain the input parameter bankfull thalweg channel depth from fully preserved channel story thickness (i.e. workflow A1), as this provides smaller uncertainty ranges than bankfull thalweg channel depth inferred from average cross-set thickness (i.e. workflow A2). Additionally, channel story thickness (i.e. workflow A1) is easily evaluated in the field and subsurface data, albeit we recommend the use of cross-set thickness (i.e. workflow A2) in case of well data, as assessment of proximity to channel axis and/or thalweg is difficult.

When establishing the updip backwater transition zone, we propose to take the bankfull thalweg depth propagated error into account but neglect the slope uncertainties (see also *6.1 Case study – ancient).* We believe this is valid approach because i) slope is generally a difficult parameter to resolve in ancient succession (Long, 2021), and different methods may result in slopes that vary up to two orders of magnitude, ii) with normal distribution, it is more likely that the relationship between grain size and slope represents steepness near the mean value than slopes far away from the mean value, iii) the case study presented here (Cretaceous Mesa Rica Sandstone, USA) shows that the updip extent of the backwater zone based on maximum backwater length estimates (Lb**, excluding uncertainty ranges resulting from slope uncertainties) does not relate to any changes in fluvial style, and occurs in an updip area with a scour depth profile tens of meters (or several channel-thicknesses) above sea-level, which is evidently outside backwater influences.

The resulting updip backwater transition zone occurs between 0.8 – 1.7 dimensionless distance for workflow A1 and 0.4 – 1.2 for workflow A2, both with respect to the mean backwater length calculated for workflow A1 (i.e. Lb = 188 km) (Fig. 9). Combining these suggest that the updip backwater transition zone most likely occurs between 0.8 to 1.3 dimensionless distance with respect to the estimated mean backwater length when taking the inherent uncertainties in obtaining bankfull thalweg depth into account. It is crucial to incorporate more studies to test and further refine the significance of an expected updip backwater transition zone.

6.2.2. Modern river systems

In modern fluvial systems, we propose and tested seven workflows to obtain backwater length estimates (Fig. 6). Of these, workflows M1–M3 apply the intersection method and Workflows M4–M7 provide backwater lengths based on Lb = h/S. The workflow recommendation is based i) accuracy, ii) application of the proposed workflows (i.e. Mississippi case study) and iii) outcomes from assessing individual aspects and methods to obtain input parameters (section 4).

We recommend to use the intersection method because it i) has the least uncertainties when obtaining direct field data (i.e. workflow M1, hydrographic surface to obtain absolute height of the riverbed profile), ii) discards the challenges of and minimizes ambiguity in obtaining slope and depth from one or a few selected locations or a certain of the river path for slope or channel depth measurements, iii) it averages the locally irregular riverbed profile over a longer section, iv) the riverbed intersection is closely related to changes in flow conditions, hydrodynamics, sedimentary trends and channel morphology (Wright & Parker, 2005; Nittrouer et al., 2011, 2012; Smith et al., 2020).

For application of workflows M4–M7, we recommend to obtain bankfull thalweg channel depth from the normal reach, or at least updip of the apex. Workflow M4 offers a convenient desktop approach, as bankfull thalweg channel depth is inferred from its empirical ratio with bankfull channel width, which can be easily obtained from satellite imagery. However, even though workflow M4 results in a backwater length closest to the actual intersection point, we believe this might be by chance as width:depth ratios are highly approximate. Based on results from the Mississippi case study (Fig. 10), we consider that the use of a cross-sectional profile (workflow M5) provides the most accurate bankfull thalweg channel depth. It is important to bear in mind that accuracy of Lb based on h/S depends on representativeness of the obtained bankfull thalweg channel depth (i.e. h) and slope (i.e. S) parameters. Additionally, application to the Mississippi river showed that resulting backwater lengths are generally short when comparing the actual riverbed intersection with sea level with backwater length estimates based on discharge and grain size (i.e. workflows M6 and M7), the latter plotting well into the non-uniform flow reach.

In summary, we recommended the following order of workflows, based on resulting backwater estimates closest to the actual intersection between riverbed and sea level in the Mississippi river case study: Workflows M1, M2 and M5. Care should be taken when applying any of the other workflows, as workflows M3 and M4 use channel width:depth ratios, which tend to be highly approximate, and workflows M6 and M7 (based on discharge and grain size, respectively) plot in the lower reaches of the backwater zone. It is crucial to incorporate more studies to test and compare backwater length estimates resulting from direct riverbed surveys combined with water elevation profiles versus backwater length estimates based on indirectly obtained parameters and the h/S approach, and eventually assess their relationship with changes in channel morphology and sedimentary trends.

6.3. Backwater estimates in modern versus ancient settings

Backwater lengths obtained in modern river systems could be a real measurement by assessing the intersection point of channel bed profiles with sea level, and the distance from that point to the river mouth. This contrasts the approach for ancient settings, in which Lb = h/S is based on parameters obtained in one or a few locations and depends on preserved proxies. The advantages of the intersection method are i) it has the least uncertainties regarding input data, ii) it discards the problem and minimizes ambiguity in obtaining slope and depth from one or a few selective locations for slope or channel depth measurements, and iii) it averages the locally irregular riverbed profile over a longer section. In ancient systems, workflows targeting the full river profile are unrealistic. Additionally, pinpointing the updip extent of the backwater zone in ancient strata is ideally linked to evidence on the coeval paleoshoreline, hence depending on accuracy of correlation, completeness of the stratigraphic record, etc. Finally, the backwater zone is a dynamic zone: its upstream extent is sensitive to river discharge as well as the water surface elevation at the river mouth, which in turn can be affected by sea level, storm surges and tides, for example. However, time is needed to adjust to such changes, and channel geometries and changes therein will represent an average when considering longer timescales.

River mouth evolution, both in direction and magnitude, matches avulsion-site migration in deltas with backwater-scaled avulsion sites (Ganti et al., 2014; Brooke et al., 2022). In ancient settings, such upstream and downstream shifting of the backwater zone could be recorded as well, as fluvial strata may record deposition throughout sea level cycles. In high accommodation systems, coastal progradation and retrogradation may be represented by downstream and upstream shifting changes in fluvial architectural style throughout a vertical succession (Shiers et al., 2018). In low-accommodation systems however, limited space may cause advancement of the fluvial system over previously deposited strata, eroding the earliest deposits related to backwater effect (Van Yperen et al., 2021). Hence, the most updip occurrence of fluvial channel fill deposits representative for backwater conditions might be representative for deposition contemporaneous to a younger shoreline.

6.4 Importance of backwater length accuracy and future work

Backwater length estimates are commonly used to assess scaling relationships with avulsion lengths (Jerolmack, 2009; Chatanantavet et al., 2012; Ganti et al., 2014, 2016; Hartley et al., 2016; Brooke et al., 2020; Prasojo et al., 2022; Brooke et al., 2022) and its relationship with changes in sedimentary trends and channel morphology (Nittrouer et al., 2011, 2012; Fernandes et al., 2016; Gugliotta et al., 2017; Smith et al., 2020) and changes in preserved fluvial strata (Colombera et al., 2016; Lin & Bhattacharya, 2017; Martin et al., 2018; Trower et al., 2018; Lin et al., 2020; van Yperen et al., 2021). The strength of these relations determine the importance of backwater length accuracy. If there is a strong correlation between backwater length, avulsion scale and changes in sedimentary trends, then it is important to get the backwater length accurate. If the relationship is weak, the accuracy becomes less relevant. Yet, this causes circular reasoning; if the estimated backwater length is possibly inaccurate, how can we testify its relation or lack thereof to other parameters?

A large proportion of studies on backwater effects focus on the potential relation between backwater length and avulsion location (Jerolmack, 2009; Chatanantavet et al., 2012; Ganti et al., 2014, 2016; Hartley et al., 2016; Chadwick et al., 2019, 2020; Brooke et al., 2020, 2022; Ratliff et al., 2021; Prasojo et al., 2022). Yet studies addressing potential relationships between the backwater effect and channel morphology, grain size trends, and fluvial-deltaic stratigraphy are less common (Nittrouer et al., 2011, 2012; Blum et al., 2013; Nittrouer, 2013; Fernandes et al., 2016; Zheng et al., 2019; Gugliotta & Saito, 2019; Smith et al., 2020; Wu & Nittrouer, 2020). Strong relationships between sedimentary trends and backwater length scale are dominantly derived from studies on the Mississippi river (e.g. Nittrouer et al., 2011, 2012; Nittrouer, 2013) and more scarcely the Trinity river (Smith et al., 2020), and Rhine river (Fernandes et al., 2016). Importantly, few studies have documented results that contrast the ‘expected’ backwater effects, such as channel widening and shallowing in tide-dominated river deltas

(Gugliotta & Saito, 2019), or absence of erosion in the distal part of the backwater zone during river floods (Zheng et al., 2019).

Additionally, there is ongoing investigation on the potential geometric scaling (i.e. without need for flood discharge variability; Chadwick et al., 2019; Ratliff et al., 2021), valley exit control (Hartley et al., 2016), bedslope changes (Prasojo et al., 2022), backwater-scaled avulsions (e.g. Ganti et al., 2016; Brooke et al., 2022). Considering results that support the later, scaling between the avulsion length and backwater length approximate a near 1:1 relationship when considering only the deltas with backwater-scaled avulsions (Brooke et al., 2022). More precisely however, their result La* = La/Lb is 0.87 ± 0.38, (La* is dimensionless avulsion length, La is avulsion length, Lb is backwater length) implies that a backwater length estimate of 300 km could relate to an avulsion node between 147 and 375 km, in addition to 37.5% of the 80 analyzed delta-plain avulsions not having a backwater-scaled avulsion. The backwater length estimates in Brooke et al. (2022) are partly based on slope and channel depth estimates that were previously published, which we demonstrated are obtained in numerous ways and therefore result in highly varying backwater lengths, making the study results less robust.

Finally, application of backwater length estimates provide an ideal tool to aid predictions in channel architecture, especially for subsurface studies. Only limited input data is needed to estimate backwater length which make it easy to get a first insight on where to expect changes in channel architectural style and grain size, and position relative to the shoreline, which is key information for reservoir and aquifer exploration.

Future work in modern river systems should further investigate the differences between backwater length estimates resulting from direct riverbed surveys combined with water elevation profiles versus backwater length estimates based on indirectly obtained parameters and the h/S approach, and eventually assess their relation to changes in channel morphology and sedimentary trends. In ancient settings, a potential link between dimensionless updip backwater transition zone and outcrop evidences for changing fluvial architectural style should be further exploited.

7. Conclusions

The backwater length is an independent measure that can be used to predict the location where channel morphology and fluvial architectural style in both modern and ancient settings, and thus reservoir characteristics, change. Common changes in the updip segment of the backwater zone are decreasing meander-bend migration rates, decreasing channel-belt width/thickness ratios, and grainsize coarsening followed by a distinct downstream fining. Previous studies show a close relation between these changes and the location where the riverbed intersects sea level, which approximates the backwater length. Only limited input data is needed to estimate backwater length, which makes it an ideal tool to aid predictions in channel architecture.

However, awareness of uncertainties involved in obtaining backwater estimates is of key importance, as different methods are used to obtain backwater length, and input parameters channel depth and slope are prone to equivocal sources and definitions, resulting in different backwater lengths for the same river systems, with up to a factor 6 differences.

We propose several workflows for both ancient and modern settings to improve uncertainty management and enhance comparability and applicability of future backwater length estimates. Workflow recommendation is based on practicality, accuracy, smallest uncertainty ranges, and allows different types of data as input parameters. For the first time, the application of multiple methods to obtain backwater length estimates are tested on a single ancient and modern river system. In ancient strata, the preferred workflow uses fully preserved single story channel fill deposits as an input parameter for bankfull thalweg channel depth, and estimates slope based on a representative grain size sample and Shields stress empirical relation. Results of this workflow closely matches changes in fluvial depositional style. In modern river systems, we recommend using the intersection method based on obtaining the absolute river bed height in the field from a hydrographic survey. Resulting backwater lengths match the river segment where before mentioned changes in channel morphology, architecture and grain size are most pronounced, whereas backwater lengths based on h/S plot downstream of this zone characterized by major changes. Special care should be taken when $L_b = h/S$

is based on grain size and discharge, as resulting estimates are less than half the distance of the riverbed intersection with sea level in the Mississippi river, and match the lower reaches of the backwater zone with minimal changes in channel morphology. If the backwater length is estimated based on h/S, we recommend obtaining bankfull thalweg channel depth from a cross-sectional profile updip of the apex.

This review is a critical step forward in openly discussing and accepting the shortcomings of applying a promising concept by listing and acknowledging the uncertainties and ambiguity in obtaining the necessary input parameters to estimate backwater lengths. Despite the uncertainties behind the estimations, the backwater concept holds potential related to predictability of changes in channel morphology and fluvial architectural style in both modern and ancient settings, with possible major applicability for improving subsurface resource exploration, aquifer management and geohazards linked to fluvial hydrodynamics.

Conflict of interest

There are no conflicts of interest for any of the authors in the preparation or publication of this work.

Data availability statement

The data that support the findings of this study are available from the corresponding author upon reasonable request.

8. Acknowledgements

This manuscript benefited from discussions with Massimiliano Ghinassi, Alvise Finotello and Valentin Zuchuat. Cody Myers is thanked for grain size analysis. The study was funded by AkerBP. Reviewers, editor and associate editor will be thanked.

9. References

Amarnath, C. R., & Thatikonda, S. (2020). Study on backwater effect due to Polavaram Dam Project under different return periods. *Water 2020, Vol. 12, Page 576*, *12*(2), 576. https://doi.org/10.3390/W12020576

Bjerklie, D. M., Birkett, C. M., Jones, J. W., Carabajal, C., Rover, J. A., Fulton, J. W., & Garambois, P. A. (2018). Satellite remote sensing estimation of river discharge: Application to the Yukon River Alaska. *Journal of Hydrology*, *561*, 1000–1018. https://doi.org/10.1016/j.jhydrol.2018.04.005

Blum, M., Martin, J., Milliken, K., & Garvin, M. (2013). Paleovalley systems: Insights from Quaternary analogs and experiments. *Earth-Science Reviews*, *116*(1), 128–169. https://doi.org/10.1016/j.earscirev.2012.09.003

Bradley, R. W., & Venditti, J. G. (2017). Reevaluating dune scalin Fig. 10. Case study on the Mississippi river: (A) Lower 1100 river km of the Mississippi River with previously published estimations of the landward extend of backwater length, and all seven workflows proposed in this study (M1–M7). ⍰ previously published backwater lengths: J = Table 1 in Jerolmack (2009), J* = Fig. 14 in Jerolmack (2009), C = Chatanatavet et al. (2012); F = Fernandes et al. (2016); H = Hartley et al. (2016), P = Prasojo et al. (2020). (B) The intersection method based on direct measurements of the riverbed (workflow M1) results in a backwater length of 680 km (modified after Nittrouer et al., 2012). Upstream of this, the thalweg channel bed slope and water surface slopes at different discharges are subequal to each other which is characteristic for normal flow reach. An updip backwater transition zone occurs between ~400 and ~700 river km (Nittrouer et al., 2012). Backwater lengths resulting from workflows M4-7 are projected onto the profile. (C) Input data, method, and resulting bankfull channel depth for each workflow. Workflow M2 was not executed as not bathymetric survey data is available. Note that workflows M4-7 are performed twice, with slope derived in the normal flow reach from the bankfull water elevation profile from gauging data (Nittrouer et al., 2011) and Digital Elevation Model (DEM). See Supplemental Table 4 for additional details. (D) and (E) illustrate a decrease in meander migration rates and channel-belt width/thickness ratio within the backwater zone. Note the abundance and absence of oxbow lakes close to the upstream limit of the backwater zone (D) and within the backwater zone (E), respectively. A further narrowing of the channel belt just downdip of inset (E) has been assigned to avulsion-driven bifurcation rather than backwater effects (Gugliotta & Saito, 2019).g relations. *Earth Science Reviews*, *165*, 356–376. https://doi.org/https://doi.org/10.1016/j.earscirev.2016.11.004

Bridge, J. S., & Tye, R. S. (2000). Interpreting the dimensions of ancient fluvial channel bars, channels, and channel belts from wireline-logs and cores. *AAPG Bulletin*, *84*(8), 1205–1228. https://doi.org/https://doi.org/10.1306/A9673C84-1738-11D7-8645000102C1865D

Brooke, S., Chadwick, A. J., Silvestre, J., Lamb, M. P., Edmonds, D. A., & Ganti, V. (2022). Where rivers jump course. *Science*, *376*(6596), 987–990. https://doi.org/DOI: 10.1126/science.abm1215

Brooke, S., Ganti, V., Chadwick, A. J., & Lamb, M. P. (2020). Flood variability determines the location of lobe-scale avulsions on deltas: Madagascar. *Geophysical Research Letters*, *47*(20). https://doi.org/10.1029/2020GL088797

Brooks, H. L., Steel, E., & Moore, M. (2022). Grain-size analysis of ancient deep-marine sediments using laser diffraction. *Frontiers in Earth Science*, *10*(564). https://doi.org/https://doi.org/10.3389/feart.2022.820866

Carey, W. C., & Keller, M. D. (1957). Systematic changes in the beds of alluvial rivers. *Journal of the Hydraulics Division1*, *83*(4), 1331–1.

Chadwick, A. J., Lamb, M. P., & Ganti, V. (2020). Accelerated river avulsion frequency on lowland deltas due to sea-level rise . *Proceedings of the National Academy of Sciences*, *117*(30), 17584–17590. https://doi.org/10.26009/s0FSLKFK

Chadwick, A. J., Lamb, M. P., Moodie, A. J., Parker, G., & Nittrouer, J. A. (2019). Origin of a preferential avulsion node on lowland river deltas. *Geophysical Research Letters*, *46*(8), 4267–4277. https://doi.org/10.1029/2019GL082491

Chatanantavet, P., Lamb, M. P., & Nittrouer, J. A. (2012). Backwater controls of avulsion location on deltas. *Geophysical Research Letters*, *39*(1). https://doi.org/10.1029/2011GL050197

Chow, V. T. (1959). *Open-channel hydraulics*. New York: McGraw-Hill.

Colombera, L., Shiers, M. N., & Mountney, N. P. (2016). Assessment of Backwater Controls On the Architecture of Distributary-Channel Fills In A Tide-Influenced Coastal-Plain Succession: Campanian Neslen Formation, U.S.A. *Journal of Sedimentary Research*, *86*(5), 476–497. https://doi.org/10.2110/jsr.2016.33

Csiki, S., & Rhoads, B. L. (2010). Hydraulic and geomorphological effects of run-of-river dams. *Progress in Physical Geography: Earth and Environment*, *34*(6). https://doi.org/10.1177/0309133310369435

Fernandes, A. M., Törnqvist, T. E., Straub, K. M., & Mohrig, D. (2016). Connecting the backwater hydraulics of coastal rivers to fluvio-deltaic sedimentology and stratigraphy. *Geology*, *44*(12), 979–982.

https://doi.org/10.1130/G37965.1

Ganti, V., Chadwick, A. J., Hassenruck-Gudipati, H. J., Fuller, B. M., & Lamb, M. P. (2016). Experimental river delta size set by multiple floods and backwater hydrodynamics. *Science Advances*, *2*(5), e1501768. https://doi.org/10.1126/sciadv.1501768

Ganti, V., Chu, Z., Lamb, M. P., Nittrouer, J. A., & Parker, G. (2014). Testing morphodynamic controls on the location and frequency of river avulsions on fans versus deltas: Huanghe (Yellow River), China. *Geophysical Research Letters*, *41*, 7882–7890. https://doi.org/https://doi.org/10.1002/2014GL061918

Graf, W. L. (1988). *Fluvial processes in dryland rivers* (1st ed.). Springer-Verlag. https://link.springer.com/book/9783540175919

Gugliotta, M., & Saito, Y. (2019). Matching trends in channel width, sinuosity, and depth along the fluvial to marine transition zone of tide-dominated river deltas: The need for a revision of depositional and hydraulic models. *Earth-Science Reviews*, *191*, 93–113. https://doi.org/10.1016/J.EARSCIREV.2019.02.002

Gugliotta, M., Saito, Y., Nguyen, V. L., Ta, T. K. O., Nakashima, R., Tamura, T., Uehara, K., Katsuki, K., & Yamamoto, S. (2017). Process regime, salinity, morphological, and sedimentary trends along the fluvial to marine transition zone of the mixed-energy Mekong River delta, Vietnam. *Continental Shelf Research*, *147*, 7–26. https://doi.org/10.1016/J.CSR.2017.03.001

Hajek, E. A., & Heller, P. L. (2012). Flow-depth scaling in alluvial architecture and nonmarine sequence stratigraphy: Example from the Castlegate Sandstone, Central Utah, U.S.A. *Journal of Sedimentary Research*, *82*(2), 121–130. https://doi.org/10.2110/JSR.2012.8

Hajek, E. A., & Wolinsky, M. A. (2012). Simplified process modeling of river avulsion and alluvial architecture: Connecting models and field data. *Sedimentary Geology*, *257*, 1–30. https://doi.org/10.1016/J.SEDGEO.2011.09.005

Hartley, A. J., Weissmann, G. S., & Scuderi, L. (2016). Controls on the apex location of large deltas. *Journal of the Geological Society*, *174*(1), 10–13. https://doi.org/10.1144/jgs2015-154

Holbrook, J. M. (1996). Complex fluvial response to low gradients at maximum regression; a genetic link between smooth sequence-boundary morphology and architecture of overlying sheet sandstone. *Journal of Sedimentary Research*, *66*(4), 713–722. https://doi.org/10.1306/D42683EC-2B26-11D7-8648000102C1865D

Holbrook, J. M. (2001). Origin, genetic interrelationships, and stratigraphy over the continuum of fluvial channel-form bounding surfaces: An illustration from middle Cretaceous strata, Southeastern Colorado. *Sedimentary Geology*, *144*(3–4), 179–222. https://doi.org/10.1016/S0037-0738(01)00118-X

Holbrook, J. M., & Wanas, H. (2014). A fulcrum approach to assessing source-to-sink mass balance using channel paleohydrologic paramaters derivable from common fluvial data sets with an example from the Cretaceous of Egypt. *Journal of Sedimentary Research*, *84*(5), 349–372. https://doi.org/10.2110/jsr.2014.29

Hudson, P. F., & Kesel, R. H. (2000). Channel migration and meander-bend curvature in the lower Mississippi River prior to major human modification | Geology | GeoScienceWorld. *Geology*, *28*(6), 531–534. https://doi.org/doi.org/10.1130/0091-7613(2000)28<531:CMAMCI>2.0.CO;2

Jerolmack, D. J. (2009). Conceptual framework for assessing the response of delta channel networks to Holocene sea level rise. *Quaternary Science Reviews*, *28*(17–18), 1786–1800. https://doi.org/10.1016/J.QUASCIREV.2009.02.015

Kimmerle, S., & Bhattacharya, J. P. (2018). Facies, backwater limits, and paleohydraulic analysis of rivers in a forced-regressive, compound incised valley, Cretaceous Ferron Sandstone, Utah, U.S.A. *Journal of Sedimentary Research*, *88*, 177–200. https://doi.org/https://doi.org/10.2110/jsr.2018.5

Knox, R. L., & Latrubesse, E. M. (2016). A geomorphic approach to the analysis of bedload and bed morphology of the Lower Mississippi River near the Old River Control Structure. Geomorphology, 268, 35–47. https://doi.org/10.1016/J.GEOMORPH.2016.05.034

Leclair, S. F., & Bridge, J. S. (2001). Quantitative interpretation of sedimentary structures formed by river dunes. *Journal of Sedimentary Research*, *71*(5), 713–716. https://doi.org/https://doi.org/10.1306/2DC40962-0E47-11D7-8643000102C1865D

Lin, W., & Bhattacharya, J. P. (2017). Estimation of source-to-sink mass balance by a fulcrum approach using channel paleohydrologic parameters of the Cretaceous Dunvegan Formation, Canada. *Journal of Sedimentary Research*, *87*(1), 97–116. https://doi.org/https://doi.org/10.2110/jsr.2017.1

Lin, W., Ferron, C., Karner, S., & Bhattacharya, J. P. (2020). Classification of paralic channel sub-environments in an ancient system using outcrops: The Cretaceous Gallup system, New Mexico, U.S.A. *Journal of Sedimentary Research*, *90*(9), 1094–1113. https://doi.org/10.2110/JSR.2019.191

Liro, M. (2019). Dam reservoir backwater as a field-scale laboratory of human-induced changes in river biogeomorphology: A review focused on gravel-bed rivers. *Science of The Total Environment*, *651*, 2899–2912. https://doi.org/10.1016/J.SCITOTENV.2018.10.138

Liro, M., Ruiz-Villanueva, V., Mikuś, P., Wyżga, B., & Bladé Castellet, E. (2020). Changes in the hydrodynamics of a mountain river induced by dam reservoir backwater. *Science of The Total Environment*, *744*(140555). https://doi.org/10.1016/J.SCITOTENV.2020.140555

Long, D. G. F. (2021). Trickling down the paleoslope: an empirical approach to paleohydrology. *Earth-Science Reviews*, *220*, 103740. https://doi.org/10.1016/J.EARSCIREV.2021.103740

Lyster, S. J., Whittaker, A. C., Hampson, G. J., Hajek, E. A., Allison, P. A., & Lathrop, B. A. (2021). Reconstructing the morphologies and hydrodynamics of ancient rivers from source to sink: Cretaceous Western Interior Basin, Utah, USA. *Sedimentology*, *68*(6), 2854–2886. https://doi.org/10.1111/sed.12877

Mackin, J. H. (1948). Concept of the graded river. *Geological Society of America Bulletin*, *59*(5), 463–512.

Martin, J., Fernandes, A. M., Pickering, J., Howes, N., Mann, S., & McNeil, K. (2018). The stratigraphically preserved signature of persistent backwater dynamics in a large paleodelta system: the Mungaroo Formation, North West Shelf, Australia. *Journal of Sedimentary Research*, *88*(7), 850–872. https://doi.org/10.2110/jsr.2018.38

Maselli, V., Pellegrini, C., Del Bianco, F., Mercorella, A., Nones, M., Crose, L., Guerrero, M., & Nittrouer, J. A. (2018). River morphodynamic evolution under dam-induced backwater: An example from the Po River (Italy). *Journal of Sedimentary Research*, *88*(10), 1190–1204. https://doi.org/10.2110/JSR.2018.61

Milliken, K. T., Blum, M. D., Snedden, J. W., & Galloway, W. E. (2018). Application of fluvial scaling relationships to reconstruct drainage-basin evolution and sediment routing for the Cretaceous and Paleocene of the Gulf of Mexico. *Geosphere*, *14*(2), 749–767. https://doi.org/10.1130/GES01374.1

Nittrouer, J. A. (2013). Backwater hydrodynamics and sediment transport in the lowermost Mississippi River Delta: Implications for the development of fluvial-deltaic landforms in a large lowland river. *Deltas: Landforms, Ecosystems, and Human Activities: International Association of Hydrological Sciences Publication*, 48–61.

Nittrouer, J. A., Lamb, M. P., & Mohrig, D. (2012). Spatial and temporal trends for water-flow velocity and bed-material sediment transport in the lower Mississippi River. *Geological Society of America Bulletin*, *124*(3–4), 400–414. https://doi.org/10.1130/B30497.1

Nittrouer, J. A., Mohrig, D., & Allison, M. (2011). Punctuated sand transport in the lowermost Mississippi River.

Journal of Geophysical Research: Earth Surface, *116*(F4), 4025. https://doi.org/10.1029/2011JF002026

Oboh-Ikuenobe, F. E., Holbrook, J. M., Scott, R. W., Akins, S. L., Evetts, M. J., Benson, D. G., & Pratt, L. M. (2008). Anatomy of epicontinental flooding: Late Albian-Early Cenomanian of the southern U.S. Western Interior Basin. In B. R. Pratt & C. Holmden (Eds.), *Dynamics of Epeiric Seas* (Issue 48, pp. 201–227). Geological Association of Canada, Special Paper. https://doi.org/10.1016/0016-7037(86)90064-5

Paola, C., & Mohrig, D. (1996). Palaeohydraulics revisited: palaeoslope estimation in coarse-grained braided rivers. *Basin Research*, *8*(3), 243–254. https://doi.org/10.1046/J.1365-2117.1996.00253.X

Parker, G. (e-book). *1-D sediment transport morphodynamics with applications to rivers and turbidity currents, e- book*. http://vtchl.uiuc.edu/people/parkerg/morphodynamics_e-book.htm

Parker, G., Wilcock, P. R., Paola, C., Dietrich, W. E., & Pitlick, J. (2007). Physical basis for quasi-universal relations describing bankfull hydraulic geometry of single-thread gravel bed rivers. *Journal of Geophysical Research: Earth Surface*, *112*(F4), 4005. https://doi.org/10.1029/2006JF000549

Pickup, G., & Rieger, W. A. (1979). A conceptual model of the relationship between channel characteristics and discharge. *Earth Surface Processes*, *4*(1), 37–42. https://doi.org/10.1002/ESP.3290040104

Pickup, G., & Warner, R. F. (1976). Effects of hydrologic regime on magnitude and frequency of dominant discharge. *Journal of Hydrology*, *29*(1–2), 51–75. https://doi.org/10.1016/0022-1694(76)90005-6

Prasojo, O. A., Hoey, T. B., Owen, A., & Williams, R. D. (2022). Slope break and avulsion locations scale consistently in global deltas. *Geophysical Research Letters*, *49*(2), e2021GL093656. https://doi.org/10.1029/2021GL093656

Ratliff, K. M., Hutton, E. W. H., & Murray, A. B. (2021). Modeling long-term delta dynamics reveals persistent geometric river avulsion locations. *Earth and Planetary Science Letters*, *559*, 116786. https://doi.org/10.1016/J.EPSL.2021.116786

Rubin, D. M., & Carter, C. L. (1987). *Cross-bedding, bedforms, and paleocurrents*. *1*, 187-undefined.

Scott, R. W., Holbrook, J. M., Oboh-Ikuenobe, F. E., Evetts, M. J., Benson, D. G., & Kues, B. S. (2004). Middle Cretaceous stratigraphy, southern Western Interior Seaway, New Mexico and Oklahoma. *Rocky Mountain Association of Geologists*, *41*(2), 33–61.

Shields, A. (1936). Anwendung der Ähnlichkeitsmechanik und der Turbulenzforschung auf die Geschiebebewegung [Application of Similarity Principles and Turbulence Research to Bed-Load Movement]. *Preußische Versuchsanstalt Für Wasserbau Und Schiffbau*, *26*, 47.

Shiers, M. N., Mountney, N. P., Hodgson, D. M., & Colombera, L. (2018). Controls on the depositional architecture of fluvial point-bar elements in a coastal-plain succession. *Fluvial Meanders and Their Sedimentary Products in the Rock Record*, 15–46. https://doi.org/10.1002/9781119424437.CH2

Smith, V., Mason, J., & Mohrig, D. (2020). Reach-scale changes in channel geometry and dynamics due to the coastal backwater effect: the lower Trinity River, Texas. *Earth Surface Processes and Landforms*, *45*(3), 565–573. https://doi.org/10.1002/ESP.4754

Surian, N., Mao, L., Giacomin, M., & Ziliani, L. (2009). Morphological effects of different channel-forming discharges in a gravel-bed river. *Earth Surface Processes and Landforms*, *34*(8), 1093–1107. https://doi.org/10.1002/ESP.1798

Trampush, S. M., Huzurbazar, S., & McElroy, B. (2014). Empirical assessment of theory for bankfull characteristics of alluvial channels. *Water Resources Research*, *50*, 9211–9220. https://doi.org/https://doi.org/10.1002/2014WR015597

Trower, E. J., Ganti, V., Fischer, W. W., & Lamb, M. P. (2018). Erosional surfaces in the Upper Cretaceous Castlegate Sandstone (Utah, USA): Sequence boundaries or autogenic scour from backwater hydrodynamics? *Geology*, *46*(8), 707–710. https://doi.org/10.1130/G40273.1

Van Yperen, A. E., Holbrook, J. M., Poyatos-Moré, M., & Midtkandal, I. (2019). Coalesced delta-front sheet-like sandstone bodies from highly avulsive distributary channels: the low-accommodation Mesa Rica Sandstone (Dakota Group, New Mexico, U.S.A.). *Journal of Sedimentary Research*, *89*(7), 654–678. https://doi.org/https://doi.org/10.2110/jsr.2019.27

van Yperen, A. E., Holbrook, J. M., Poyatos-Moré, M., Myers, C., & Midtkandal, I. (2021). Low-accommodation and backwater effects on sequence stratigraphic surfaces and depositional architecture of fluvio-deltaic settings (Cretaceous Mesa Rica Sandstone, Dakota Group, USA). *Basin Research*, *33*(1), 513–543. https://doi.org/10.1111/bre.12483

Williams, G. P. (1978). Bankfull discharge of rivers. *Water Resources Research1*, *14*, 1141–1158.

Wright, S., & Parker, G. (2005). Modeling downstream fining in sand-bed rivers. I: Formulation. *Journal of Hydraulic Research*, *43*(6), 613–620. https://doi.org/10.1080/00221680509500381

Wu, C., & Nittrouer, J. A. (2020). Impacts of backwater hydrodynamics on fluvial–deltaic stratigraphy. *Basin Research*, *32*(3), 567–584. https://doi.org/10.1111/BRE.12385/CITE/REFWORKS

Yalin, M. S. (1964). Geometrical properties of sand waves. *Journal of the Hydraulics Division*, *90*(5), 105–119.

https://doi.org/10.1061/JYCEAJ.0001097

Zheng, S., Edmonds, D. A., Wu, B., & Han, S. (2019). Backwater controls on the evolution and avulsion of the Qingshuigou channel on the Yellow River Delta. *Geomorphology*, *333*, 137–151. https://doi.org/https://doi.org/10.1016/j.geomorph.2019.02.032

Supplemental Text S1 – Extensive caption for Figure 3

A – C (reference to section 4.1. and 4.2. in text). Here we assess the impact of using different segments of the river system to obtain either slope (A) or channel depth (B). (A) To illustrate how different slopes impact the resulting backwater length, we keep the channel depth constant and use a bankfull thalweg depth of 31 m for each Lb estimate (i.e. thalweg channel depth at 650 river km, Fig. 2 in Nittrouer et al., 2011). All slope estimates are derived from water level elevation heights from the mean water elevation profile in Nittrouer et al. (2011). Location 1-4 are depicted in C. ⧫It is unclear whether Paola & Mohrig (1996) include the lower reaches of a river system. (B) To illustrate how different depths impact the resulting backwater length, we ensure that only the location is the only variable when obtaining slope. All river depths are obtained from the Mississippi river thalweg depth bathymetric profile at high discharge (Nittrouer et al., 2011) to ensure the same method and type of channel depth is used (see 4.3. and 4.4.). ** Estimated with intersection method based on riverbed profile and water level elevation data. (C) Southern Louisiana and the Mississippi river. The yellow circle indicates the apex and avulsion node with the Atchafalaya river. White circles are depicted with a 200 river-kilometer spacing. Note how straight-line distances (in Italics) to Head of Passes are significantly shorter than distances measured in river km.

D (reference to section 4.3. in text). Different types of channel depth for the Mississippi river result in different channel depths and hence different backwater length estimates. Here, backwater (Lb) estimates are calculated based on Lb = h/s and we use a slope of $6.75*10^{-5}$ is for each Lb estimate, to illustrate how different types of channel depths impact the resulting backwater length. 1) Bankfull thalweg depth at times of water level a (i.e. bankfull water level), 2) Average depth, linked to water level b (i.e. normal flow / mean flow / characteristic flow) (= bankfull thalweg depth / 1.48 in Bjerklie et al., 2018), 3) Average bankfull is obtained differently by different authors. Here, average bankfull depth = (bankfull thalweg / 1.502)$^{(1/0.9603)}$ in Long (2021), which approximates dashed-line 3. 4) Average bankfull depth as one-half of the maximum bankfull thalweg depth (Bridge & Tye, 2000; Leclair & Bridge, 2001; Holbrook & Wanas, 2014), which approximates dashed-line 4.

E (reference to section 4.4. in text). Different methods to obtain bankfull thalweg depth for the Mississippi river result in different channel depths and hence different backwater length estimates. Here, backwater (Lb) estimates are calculated based on Lb = h/s and we use a slope of 6.75*10-5 for each Lb estimate, to illustrate how different channel depths impact the resulting backwater length. Using this slope causes a difference between the listed channel depths based on river discharge and literature in this table and their respective references because other slope values were used in these publications. See Supplemental table 2 for more information on slopes used in previous publications for backwater length estimates on the Mississippi river.

F (reference to section 4.5. in text). Obtaining slope estimates from either digital elevation models or gauging data at bankfull stages gives different results, for the Mississippi river in the normal flow reach. Previously published slope estimates based on digital elevation models were not used as these are based on different reaches or unspecified. Here, backwater (Lb) estimates are calculated based on Lb = h/s and we use a depth of 31 m for each Lb estimate (Fig 2 in Nittrouer et al., 2011), to illustrate how different slope estimates impact the resulting backwater length.

Supplemental Text S2 – Calculating and displaying errors

In geoscience literature, uncertainties are often expressed in a mixture of uncertainty factors and percent errors (e.g. Di Baldassarre et al., 2013; Holbrook & Wanas, 2014; Lyster et al., 2022) with these should be approached differently.

S2.1 Calculating with uncertainty factors

Uncertainty factors are used for the factor by which the measured value is multiplied and divided in order to generate the limits of a confidence interval. This results in asymmetric confidence intervals and the lower limit of the confidence interval for values near zero will not be negative (Ramsey & Ellison, 2015). Uncertainty factor: an alternative way to express measurement uncertainty in chemical measurement). Uncertainty factors are annotated with both minimum and maximum ranges, e.g. an uncertainty factor of ± 4.

Upper limit taking into account a known uncertainty factor = real value x uncertainty factor

Lower limit taking into account a known uncertainty factor = real value / uncertainty factor

Example given: A channel width of 100 m with an error factor of ± 4 gives a 100 x 4 = 400 m maximum value, and a 100 / 4 = 25 m minimum value.

Factors smaller than 1 are typically treated as percentages or relative error.

S2.2 Calculating with a known relative error

Relative errors and percent errors tend to have symmetric confidence intervals.

Relative error = (measured – real) / real

Percent error = ((measured – real) / real)) x 100

Upper limit taking into account a known error = real value + (relative error x real value)

Lower limit taking into account a known error = real value – (relative error x real value)

Example given: A 10 m thick channel with a relative error of ± 0.25, gives a 10 + (0.25 x 10) = 12.5 m maximum value, and a 10 – (0.25 x 10) = 7.5 minimum value.

Supplemental Text S3 – Calculation details for individual error estimates in ancient settings

Step A) (channel storey thickness) is considered to have a 25% error, based on potential for miss-identification of complete channel-fill storey thickness (Holbrook & Wanas, 2014).

- A 25% error translates to a relative error of ± 0.25

Step B) (compaction factor) has an error range that is unidirectional as decompaction only applies in one direction. A compaction factor of 1.1 is commonly used (Holbrook & Wanas, 2014; Long, 2021), but it is important to acknowledge that the likely range is between 1.0 and 1.69 (Long, 2021).

- 0 to 0.69 is the relative error range.

Step C) (dune height): h_d = 2.9(±0.7)$h_{xs\text{-}mean}$ (Leclair & Bridge, 2001), with h_d = mean dune height and $h_{xs\text{-}mean}$ = mean cross-set height.

- We use an example calculation to obtain the relative errors. Example given for a mean cross set thickness of 0.5 m. The mean value is: 2.9 x 0.5 = 1.45 m. The maximum value is (2.9 + 0.7) x 0.5 = 1.8 m. The minimum value is (2.9 – 0.7) x 0.5 = 1.1 m.
- The relative error is calculated following:

  Positive relative error: (max – mean) / mean = relative error →(1.8-1.45)/1.45 = 0.24

  Negative relative error: (mean – min) / mean = relative error →(1.45-1.1)/1.45 = 0.24
- The relative error is ± 0.24

Step D) (Formative flow depth): $H = 6.7h_d$, with (H) = formative flow depth and (h_d) = mean dune height. There is a 50% chance that H is between 4.4 h_d and 10 h_d (Bradley & Venditti, 2017).

We use an example calculation to obtain the relative errors. Example given for a mean dune height of 1 m. The mean value is: 6.7 x 1 = 6.7 m. The maximum value is 10 x 1 = 10 m. The minimum value is 4.4 x 1 = 4.4 m

- The relative error is calculated following:

Positive relative error: (max – mean) / mean = relative error →(10-6.7)/6.7 = 0.49

Negative relative error: (mean – min) / mean = relative error →(6.7-4.4)/6.7 = 0.34

- The relative error is +0.49 and -0.34

Step E) (Representative grain size sample). Selecting a representative grain size sample (step e) is considered to have a 50% error, based on common challenges when identifying representative bedload samples in outcrop and core data (Holbrook & Wanas, 2014).

- A 50% error translates to a relative error of ± 0.5

Step F) (Slope based on Shields stress) is considered to have an uncertainty factor of ± 2

Step G) (Channel width) is considered to have an uncertainty factor of ± 4 (Holbrook & Wanas, 2014).

Step (H) (Slope based on Channel width): $S = 0.0341 \times w_{bf}^{-0.7430}$ (Long, 2021), with W_{bf} is bankfull channel depth. SD = 0.50, n = 2295.

- The 95% confidence interval can be calculated with: $\bar{x} \pm z^* \sigma/\sqrt{n}$, where $\bar{x}$ is the sample mean, σ is the population standard deviation, n is the sample size, and z^* represents the appropriate z^*-value (1.96 for a confidence level of 95%).
- Based on a sample mean of 10-3, the 95% confidence interval is 0.021. This results in an uncertainty factor of ± 21

Extra: error in empirical equation proposed by Long (2021) to estimate paleoslope: $S = 0.0239 (D50/d_{bf})^{0.4763}$ with D50 and d_{bf} (bankfull thalweg channel depth) in mm. SD = 0.46, n = 1158

- The 95% confidence interval can be calculated with: $\bar{x} \pm z^* \sigma/\sqrt{n}$, where $\bar{x}$ is the sample mean, σ is the population standard deviation, n is the sample size, and z^* represents the appropriate z^*-value (1.96 for a confidence level of 95%).

- Based on a sample mean of 10-3, the 95% confidence interval is 0.027. This results in an uncertainty factor of ± 27

Supplemental Text S4 – Cumulative uncertainties and error propagation

Each workflow involves multiple sources of error that propagate through the backwater length calculation and therefor effect the output.

The cumulative relative uncertainty can be calculated by:

$$\frac{\Delta Q}{|Q|} = \sqrt{\left(\frac{\Delta a}{\mathrm{a}}\right)^2 + \left(\frac{\Delta \mathrm{b}}{\mathrm{b}}\right)^2 + \cdots + \left(\frac{\Delta z}{\mathrm{z}}\right)^2}$$

where Δa/a, Δb/b, etc are the relative errors inherent to the steps included.

From this follows that the cumulative absolute error is:

$$\Delta Q = Q \times \sqrt{\left(\frac{\Delta a}{\mathrm{a}}\right)^2 + \left(\frac{\Delta \mathrm{b}}{\mathrm{b}}\right)^2 + \cdots + \left(\frac{\Delta z}{\mathrm{z}}\right)^2}$$

In the outcrop case study, we take the following steps to estimate the cumulative uncertainty:

1) $\left(\frac{\Delta a}{\mathrm{a}}\right)^2 + \left(\frac{\Delta \mathrm{b}}{\mathrm{b}}\right)^2 + \cdots + \left(\frac{\Delta z}{\mathrm{z}}\right)^2 = \frac{\Delta Q}{|Q|}^2$ where Δa/a, Δb/b, etc are the relative errors inherent to the steps included in the different workflows.

Note that this equation is based on relative errors, but some of the uncertainties are expressed in factors. Therefore, these need to be converted to relative errors. Relative error = (measured – real) / real.

Example given: the uncertainty factor +- 4 for a channel width of 10 m

- Upper limit: 10 x 4 = 40 m. The relative error (instead of uncertainty factor) for the upper limit is (40 – 10) / 10 = 3. (the % error would be 300).
- Lower limit: 10 / 4 = 2.5 m. The relative error (instead of uncertainty factor) for the lower limit is (10 – 2.5) / 10 = 0.75
- Verification: Upper limit taking into account a known error = real value + (relative error x real value) → 10 + (3 x 10) = 40 m
- Verification: Lower limit taking into account a known error = real value – (relative error x real value) → 10 – (0.75 x 10) = 2.5 m

Example given: the uncertainty factor +- 2 for slope based on Shields stress for a grainsize 0.22

- Upper limit: 0.22 x 2 = 0.44 mm. The relative error (instead of uncertainty factor) for the upper limit is (0.44 – 0.22) / 0.22 = 1 (the % error would be 100).
- Lower limit: 0.22 / 2 = 0.11 mm. The relative error (instead of uncertainty factor) for the lower limit is (0.22 – 0.11) / 0.22 = 0.5
- Verification: Upper limit taking into account a known error = real value + (relative error x real value) → 0.22 + (1 x 0.22) = 0.44 mm
- Verification: Lower limit taking into account a known error = real value – (relative error x real value) → 0.22 – (0.5 x 0.22) = 0.11 mm

Example given: the uncertainty factor +- 21 for slope based on channel width for a channel 100 m wide:

- Upper limit: 100 x 21 = 2100 m. The relative error (instead of uncertainty factor) for the upper limit is (2100 – 100) / 100 = 20 (the % error would be 2000).
- Lower limit: 100 / 21 = 4.76 m. The relative error (instead of uncertainty factor) for the lower limit is (100 – 4.76) / 100 = 0.95
- Verification: Upper limit taking into account a known error = real value + (relative error x real value) → 100 + (20 x 100) = 2100 m

- Verification: Lower limit taking into account a known error = real value – (relative error x real value) → 100 – (0.95 x 100) = 5 m

2) $\sqrt{\left(\frac{\Delta a}{\mathrm{a}}\right)^2 + \left(\frac{\Delta \mathrm{b}}{\mathrm{b}}\right)^2 + \cdots + \left(\frac{\Delta z}{\mathrm{z}}\right)^2} = \frac{\Delta Q}{|Q|}$ calculates the relative cumulative error

3) $Q \times \sqrt{\left(\frac{\Delta a}{\mathrm{a}}\right)^2 + \left(\frac{\Delta \mathrm{b}}{\mathrm{b}}\right)^2 + \cdots + \left(\frac{\Delta z}{\mathrm{z}}\right)^2} = \Delta Q$ calculates the absolute error

References

Bjerklie, D. M., Birkett, C. M., Jones, J. W., Carabajal, C., Rover, J. A., Fulton, J. W., & Garambois, P. A. (2018). Satellite remote sensing estimation of river discharge: Application to the Yukon River Alaska. *Journal of Hydrology*, *561*, 1000–1018. https://doi.org/10.1016/j.jhydrol.2018.04.005

Bradley, R. W., & Venditti, J. G. (2017). Reevaluating dune scaling relations. *Earth Science Reviews*, *165*, 356–376. https://doi.org/https://doi.org/10.1016/j.earscirev.2016.11.004

Bridge, J. S., & Tye, R. S. (2000). Interpreting the dimensions of ancient fluvial channel bars, channels, and channel belts from wireline-logs and cores. *AAPG Bulletin*, *84*(8), 1205–1228. https://doi.org/https://doi.org/10.1306/A9673C84-1738-11D7-8645000102C1865D

Di Baldassarre, G., Kooy, M., Kemerink, J. S., & Brandimarte, L. (2013). Towards understanding the dynamic behaviour of floodplains as human-water systems. *Hydrology and Earth System Sciences*, *17*(8), 3235–3244. https://doi.org/10.5194/hess-17-3235-2013

Holbrook, J. M., & Wanas, H. (2014). A fulcrum approach to assessing source-to-sink mass balance using channel paleohydrologic paramaters derivable from common fluvial data sets with an example from the Cretaceous of Egypt. *Journal of Sedimentary Research*, *84*(5), 349–372. https://doi.org/10.2110/jsr.2014.29

Leclair, S. F., & Bridge, J. S. (2001). Quantitative interpretation of sedimentary structures formed by river dunes. *Journal of Sedimentary Research*, *71*(5), 713–716. https://doi.org/https://doi.org/10.1306/2DC40962-0E47-11D7-8643000102C1865D

Long, D. G. F. (2021). Trickling down the paleoslope: an empirical approach to paleohydrology. *Earth-Science*

Reviews, *220*, 103740. https://doi.org/10.1016/J.EARSCIREV.2021.103740

Lyster, S. J., Whittaker, A. C., Hajek, E. A., & Ganti, V. (2022). Field evidence for disequilibrium dynamics in preserved fluvial cross-strata: A record of discharge variability or morphodynamic hierarchy? *Earth and Planetary Science Letters*, *579*, 117355. https://doi.org/10.1016/j.epsl.2021.117355

Nittrouer, J. A., Mohrig, D., & Allison, M. (2011). Punctuated sand transport in the lowermost Mississippi River. *Journal of Geophysical Research: Earth Surface*, *116*(F4), 4025. https://doi.org/10.1029/2011JF002026

Paola, C., & Mohrig, D. (1996). Palaeohydraulics revisited: palaeoslope estimation in coarse-grained braided rivers. *Basin Research*, *8*(3), 243–254. https://doi.org/10.1046/J.1365-2117.1996.00253.X

Ramsey, M. H., & Ellison, S. L. R. (2015). Uncertainty factor: an alternative way to express measurement uncertainty in chemical measurement. *Accreditation and Quality Assurance*, *20*, 153–155. https://doi.org/10.1007/s00769-015-1115-6

Table S1. Channel depth (m) as listed in different publications used to estimate backwater lengths. Note that authors use different methods to obtain channel depth and use different types of channel depth (e.g. bankfull vs average channel depth

River	Country	Prasojo et al. 2022***	Hartley et al. 2016	Jerolmack 2009	Chatanantavet et al. 2012	Brooke et al. 2022	Nittrouer et al. 2011	Fernandes et al. 2016	Ganti et al. 2014	Gugliotta et al. 2017
Amazon	Brazil	-	45	-	12	-	-	-	-	-
Brahmaputra	Bangladesh	-	15	7	-	-	-	-	-	-
Danube	Romania	18	-	-	6	6*	-	-	-	-
Ebro	Spain	5	-	-	-	-	-	-	-	-
Magdalena	Colombia	9	-	6	6	6*	-	-	-	-
Manitoba	Canada	-	-	-	4	-	-	-	-	-
Mekong	Vietnam, Cam	13	23	-	-	-	-	-	-	◆
Mississippi	USA	20	25	25	21	*21	◆	18, 21, 24	-	-
Niger	Nigeria	10	15	-	-	-	-	-	-	-
Nile	Egypt	6	16	-	16	16*	-	-	-	-
Orinoco	Venezuela	24	12	12	8	8*	-	-	-	-
Paraná	Argentina	-	20	7	12	12*	-	-	-	-
Rhine-Meuse	Netherlands	-	-	-	5	5*	-	6, 8, 10**	-	-
Rhône	France	4	11	5	-	-	-	-	-	-
Volga	Russia	11	-	6	-	-	-	-	-	-
Zambezi	Mozambique	6	12	-	-	-	-	-	-	-
Huange / Yell	China	-	3	2	-	3*	-	-	2-5	-

*** depth not listed in Prasojo 2022 but calculated based on the formula listed in their publication based on discharge
◆ used intersection method with river bed profile and water level elevation data
** for the Nederrijn-Lek and Linge chanel belts
* from previous publications. See Brooke et al. 2022 table S1

Table S2. Slope as listed in different publications used to estimate backwater lengths. Note that authors use different methods to obtain slope

River	Country	Prasojo et al. 2022 ♦	Hartley et al. 2016 ♦	Jerolmack 2009 ¥	Chatanantavet et al. 2012 ¥	Brooke et al. 2022 ♦	Nittrouer et al. 2011 ■	Fernandes et al. 2016 ■❖	Ganti et al. 2014 ¥	Gugliotta et al. 2017 ❖
Amazon	Brazil	-	2,31E-05	-	3,0E-05	-	-	-	-	-
Brahmaputra	Bangladesh	-	5,40E-05	1,1E-04	-	-	-	-	-	-
Danube	Romania	1,19E-05	-	-	5,0E-05	5.0E-05*	-	-	-	-
Ebro	Spain	2,78E-04	-	-	-	-	-	-	-	-
Magdalena	Colombia	5,12E-05	-	9,5E-05	9,5E-05	9.5E-05*	-	-	-	-
Manitoba	Canada	-	-	-	5,0E-04	-	-	-	-	-
Mekong	Vietnam, Cam	1,87E-05	2,89E-05	-	-	-	-	-	-	intersection
Mississippi	USA	6,02E-05	2,97E-05	3,0E-05	4,3E-05	4.3E-05*	2.0E-05 - 4.0E-5	6,0E-05	-	-
Niger	Nigeria	9,18E-05	5,87E-05	-	-	-	-	-	-	-
Nile	Egypt	6,86E-05	4,76E-05	-	6,4E-05	6.4E-05*	-	-	-	-
Orinoco	Venezuela	4,13E-05	5,01E-05	6,0E-05	6,0E-05	6.0E-05*	-	-	-	-
Paraná	Argentina	-	4,43E-05	9,6E-05	4,0E-05	4.0E-05*	-	-	-	-
Rhine-Meuse	Netherlands	-	-	1,1E-04	1,1E-04	1.1E-04*	-	1.1E-04**	-	-
Rhône	France	3,82E-04	1,35E-04	4,0E-05	-	-	-	-	-	-
Volga	Russia	5,80E-05	-	-	-	-	-	-	-	-
Zambezi	Mozambique	2,53E-04	1,68E-04	-	-	-	-	-	-	-
Huange / Yellc	China	-	1,19E-04	2,0E-04	-	6.4E-05*	-	-	8,8E-05 - 1,0E-4	-

♦ Slope estimate obtained from DEM ■ Slope estimate from direct measurement of water level or river bed elevation ❖other method ¥ unclear

* from previous publications. See Brooke et al. 2022 table S1

** for the Nederrijn-Lek and Linge chanel belts

Table S3A (Fig. 3A) Assessing the impact of using different segments of the river system to obtain slope. The channel depth is kept constant. Note how a slope obtained between the apex and shoreline gives the longest backwater length. Location 1-4 are depicted in C. ♦It is unclear whether Paola & Mohrig (1996) include the lower reaches of a river system. Note: a slope of 6.75*10-5 is used for each Lb estimate, to allow for comparison. Therefore, resulting channel depths listed here may differ from their respective reference, as these references may have used different slopes. Sedimenty density and D50 (Knox & Latrubesse, 2016). D50 is based on grainsize estimates at approximately 500 river kilometers from the coastline (Knox & latrubesse 2016) represents fine to medium sand.

Location to obtain input parameters						
Slope						
Input					**Output**	
Input location	**Selected reference***	**Input parameters based on bankfull discharge**		**Channel depth (m)**	**Slope**	**Backwater length (km)**
1. Between apex and shoreline	This study, following Hartley et al. 2016	19 m elevation at 490 river km	0 m elevation at 0 river km	31	3,88E-05	799
2. Normal flow reach	This study, following Fernandes et al. 2016	53 m elevation at 1050 river km	26 m elevation at 650 river km	31	6,75E-05	459
3. Upstream of avulsion site, across 25 km	This study, following Brooke et al. 2020	20 m elevation at 515 river km	19 m elevation at 490 river km	31	4,00E-05	775
4. Distances long compared to backwater length ♦	This study, following Paola and Mohrig 2009 ♦	54 m elevation at 1050 river km	0 m elevation at 0 river km	31	5,14E-05	603

Table S3B (Fig. 3B) Assessing the impact of using different segments of the river system to obtain channel depth. The slope is kept constant. **Note how all estimates result in backwater lengths shorter than with the intersection method by Nittrouer et al. (2011). All river depths are obtained from the bathymetric profile of the Mississippi thalweg channel depth (Nittrouer et al., 2011) to ensure the same method and type of channel depth is used (see 3.3 and 3.4). In that case, only the location to obtain this input parameter varies. The Mississippi apex is around 490 river km (Chatanantavet et al., 2012).

Location to obtain input parameters				
Depth				
Input			**Output**	
Input location	**Selected reference***	**Slope**	**Channel depth (m)**	**Backwater length (km)**
Upstream of backwater zone	This study, following Chatanantavet et al. 2012	6,75E-05	26	385
Upstream of avulsion site	This study, following Brooke et al. 2020	6,75E-05	27	400
As close to the upstream limit of the delta as data availability allows	This study, following Prasojo et al. 2022	6,75E-05	29	430
Apex	This study, following Ganti et al. 2004	6,75E-05	29	430
Average depth over distances long compared to bac	This study, following Paola and Mohrig 2009	6,75E-05	31	459
Continuously, lower 1050 river kilometers	Nittrouer et al. 2011	6,75E-05	variable along river path	680**

Table S3C (Fig. 3C) Assessing the impact of different types of channel depth for the Mississippi river and how this results in different channel depths and hence different backwater length estimates. Here, backwater (Lb) estimates are calculated based on Lb = h/s and we use a slope of 6.75*10-5 is for each Lb estimate. Apex = 490 river km. Normal flow reach is from 650 km upstream. Depth is chosen based on thalweg depth at 650 river km (Nittrouer et al., 2011).

Different types of channel depth				
Input			**Output**	
Type of channel depth	**Selected reference***	**Slope**	**Channel depth (m)**	**Backwater length (km)**
1. Bankfull thalweg	Nittrouer et al. 2011	6,75E-05	31	459
2. Average depth (equals mean flow depth)	This study, following Bjerklie et al. 2018	6,75E-05	21	419
3. Average bankfull	This study, following Long 2021	6,75E-05	23	468
4. Average bankfull	This study, following Bridge & Tye 2000	6,75E-05	15,5	310

Table S3D (Fig. 3E) Assessing the impact of different methods to obtain bankfull thalweg depth for the Mississippi river and how this results in different channel depths and hence different backwater length estimates. Note how resulting backwater lengths vary between 256 km and 680 km.

Methods to obtain bankfull thalweg depth					
Input				**Output**	
Type of channel depth	**Selected reference***	**Input parameters**	**Slope**	**Channel depth (m)**	**Backwater length (km)**
Direct; riverbed survey	Nittrouer et al. 2011	River bed profile	6,75E-05	variable along river path	680**
Shields stress	This study - Mississippi river (used in Brooke et al. 2020 for rivers in Madagascar)	τ^*_{bf50} =(d_mS)/(PD_{50}). D_m = mean bankfull channel depth, S = slope = 6.75*10-5, P = submerged dimensionless density = 1.65 g/cm3, D_{50} = average grainsize for lowermost portion of the channel = 280 µm, τ_{bf50}= Shields number for dimensionless shear stress = 1.86. The resultig mean bankfull chanel depth (15 m) needs to be converted to obtain bankfull thalweg channel depth with formula 7.	6,75E-05	17	256
River discharge	Prasojo et al. 2022	characteristic flow depth h_c = ($C_f Q_c^2 / g W_{av}^2 S$)^1/3 (*sensu* Parker, 2007). C_f = bed friction coefficient = 0.002, Q_c = characteristic water discharge = 33385 m3/s, W_{av} = channel width = 669 m, g = gravitational acceleration = 9.8 m/s2, S = slope = 6.75*10-5.	6,75E-05	20	290
Channel deposits	Fernandes et al. 2016	Filled oxbow lake deposits	6,75E-05	21	311
Literature	Hartley et al. 2016	Published information or *"reliable depth measurements for portions of the river close to the apex were used"*	6,75E-05	25	500

Table S3E (Fig. 3F) Obtaining slope estimates from either digital elevation models or gauging data at bankfull stages gives different results for the Mississippi river in the normal flow reach. We use a depth of 31 m for each Lb estimate (Fig 2 in Nittrouer et al. 2011), to illustrate how different slope estimates impact the resulting backwater length. For both methods, slopes were obtained in the normal flow reach, and therefore were not dirrectly coppied from previously published slopes obtained from digital elevation models, as different reaches were used or undefined. In order to ensure that the same location (see 3.1) was used to obtain slope estimates, we obtained them from the normal didn't use directly the slope estimates published 3.0 x 10-5 (Jerolmack, 2009; Hartley et al., 2016) and 6.0 x 10-5 (Prasojo et al., 2022) .

Method to obtain slope				
Input			**Output**	
Input data	**Selected reference***	**Channel depth (m)**	**Slope**	**Backwater length (km)**
Gauging data: water elevation profile	Fig 2 in Nittrouer et al. 2011	31	6,75E-05	459
Digital elevation model	Following Hartley et al. 2016	31	8,50E-05	365

Table S4. Case study with application of all proposed workflows to obtain backwater length estimates in ancient settings (A1-4). All workflows utilize input parameters obtained from the Cretaceous Dakota Group (USA) (Van Yperen et al., 2021)
Letters between brackets (e.g. (A)) refer to calculation steps and their respective uncertainties discussed in text. * = including propagated errors in obtaining channel depth and slope. ** = including propagated errors in obtaining channel depth. ♦ = non-dimensionelized backwater length (Lb) with respect to 188 km (i.e. mean backwater length for workflow 1) by multiplication of propagated errors of both channel depth and slope. ♦♦ non-dimensionelized backwater length (Lb) with respect to188 km (i.e. mean backwater length for workflow 1) by multiplication of propagated errors of only channel depth

Bankfull thalweg channel depth

Input data		obtaining channel thickness (A) relative error		decompaction factor (B) relative error				statistical parameter (Δ_Q^2/Q^2)		cumulative uncertainty relative error (Δ_Q/Q)	absolute error (Δ_Q)	Output Channel thickness (m)	
One storey channel thickness (m)	**12**											mean value (Q)	13,2
		positive	0,25	positive	0,69			positive	0,54	0,73	9,7	max	22,9
		negative	-0,25	negative	0			negative	0,06	0,25	3,3	min	9,9
Input data		**decompaction factor (B) relative error**		**dune height (C) relative error**		**bankfull thalweg depth (D) relative error**		**statistical parameter (Δ_Q^2/Q^2)**		**cumulative uncertainty relative error (Δ_Q/Q)**	**absolute error (Δ_Q)**	**Output Channel thickness (m)**	
Average cross-set thickness (m)	**0,49**											mean value (Q)	10,5
of lower beds representative for formative flow...		positive	0,69	positive	0,24	max	0,49	positive	0,77	0,88	9,2	max	19,7
		negative	0	negative	-0,24	min	-0,34	negative	0,17	0,42	4,4	min	6,1

Slope

Input data		grainsize sample (e) relative error		slope (grainsize & Shields stress) (f) relative error		statistical parameters (Δ_Q^2/Q^2)		cumulative uncertainty relative error (Δ_Q/Q)	absolute error (Δ_Q)	Output Slope - channel depth workflow 1		Output Slope - channel depth	
Grainsize (mm)	**0,22**									mean value (Q)	7,02E-05	mean valu	8,94E-05
		positive	0,5	positive	2,0	positive	4,25	2,06	1,45E-04	max	2,15E-04	max	2,34E-04
		negative	-0,5	negative	0,5	negative	0,50	0,71	4,97E-05	min	2,06E-05	min	3,97E-05
Input data		**channel width (g) relative error**		**slope (channel width) (h) relative error**		**statistical parameters (Δ_Q^2/Q^2)**		**cumulative uncertainty relative error (Δ_Q/Q)**	**absolute error (Δ_Q)**	**Output Slope**			
Channel width (m)	**250**									mean value (Q)	5,64E-04		
		positive	3,0	positive	21,0	positive	450	21,21	1,20E-02	max	1,25E-02		
		negative	0,75	negative	4,76	negative	23,24	4,82	1,17E-04	min	4,47E-04		

note: because here the cumulative error is more than 1 for the negative, we treat it as a factor (which means the absolute error is calculated by mean value / relative error instead of mean value * relative error).

Workflow calculations backwater (Lb)

Input data			channel (m) relative error	slope relative error	statistical parameter (Δ_Q^2/Q^2)		cumulative uncertainty relative error (Δ_Q/Q)	absolute error (Δ_Q)	Output - Lb (km)	Lb (km)* (errors h &	Lb (km)** error h	Output - Lb dimensionless r/Lb*	r/Lb**
Workflow A1 (channel storey & grain size)									mean value (Q)	188	188	1,0	1,0
input data channel thickness	13,2	max	0,73	2,06	max	4,79	2,19	411,32	max	599	326	3,2	1,7
input data slope	7,02E-05	min	0,25	0,71	min	0,56	0,75	140,97	min	47	141	0,3	0,8
Workflow A2 (crossbed thickness & grain size)									mean value (Q)	117	117	0,6	0,6
input data crossbed thickness	10,5	max	0,88	2,06	max	5,02	2,24	262,67	max	380	220	2,0	1,2
input data slope	8,94E-05	min	0,42	0,71	min	0,67	0,82	0,82	min	116	68	0,6	0,4
Workflow A3 (channel storey & channel width)									mean value (Q)	23	23	0,1	0,1
input data channel thickness	13,2	max	0,73	21,21	max	450,54	21,23	497,00	max	520	41	2,8	0,2
input data slope	5,64E-04	min	0,25	4,82	min	23,30	4,83	113,02	min	-90	18	-0,5	0,1
Workflow A4 (crossbed thickness & channel width)									mean value (Q)	19	19	0,1	0,1
input data crossbed thickness	10,5	max	0,88	21,21	max	450,77	21,23	394,42	max	413	35	2,2	0,2
input data slope	5,64E-04	min	0,42	4,82	min	23,41	4,84	89,89	min	-71	11	-0,4	0,1

	formula used - see manuscript	multiplier for expected value
obtaining channel thickness (A)	-	1
decompaction (B)	-	1,1
dune height (C)	formula 1	2,9
bankfull thalweg depth (D)	formula 2	6,7

Slope based on Shields stress (e.g. Holbrook and Wanas, 2014)

Slope = $(\tau \times (RD_{50}) / H$

τ*bf50 Shields stress	1,86
Submerged Density (g/cm^3)	1,65
Mesa Rica Sandstone D50 (m)	2,20E-04
H bankfull channel depth - workflow 1	13,2
average bankfull channel depth (following Lo	9,6
H bankfull channel depth - workflow 2	10,5
average bankfull channel depth (following Lo	7,6
Slope: average grain size - workflow 1	7,02E-05
Slope: average grain size - workflow 2	8,94E-05

Slope based on channel width (Long, 2021)

Slope = 0.0341*Wbf^-0.7430
Wbf = bankfull channel width

Slope: average channel width 5,64E-04

Table S5. Case study with application of all proposed workflows to obtain backwater length estimates in moddern settings (M1-7), applied on the Mississippi River.

Workflow calculations backwater (Lb) - Modern case study		Output								additional info		
Input data	Method	slope from water elevation profile				slope from DEM						
		depth (m)	slope	Lb (km)	r/Lb	depth (m)	slope	Lb (km)	r/Lb	Selected reference for method*	formula	input parameters
Workflow M1 (river bed survey)	*intersection*	-	-	680	1	-	-	-	-	Nittrouer et al. 2012		
Workflow M2 (bathymetric survey)	*intersection*	-	-	-	-	-	-	-	-			
Workflow M3 (channel width)	*intersection*	-	-	800	1,2	-	-	-	-	this study		
Workflow M4 (channel width)	*Lb = h/S*	33	6,75E-05	491	0,7	33	8,50E-05	390	0,6	Long, 2021	Bankfull channel width = 16.872*depth^1.169 --> depth = (width / 16.872)^(1/1.169)	width around apex is 1010 m
Workflow M5 (cross section)	*Lb = h/S*	29	6,75E-05	430	0,6	29	8,50E-05	341	0,5	Nittrouer et al. 2011		
Workflow M6 (discharge)	*Lb = h/S*	20	6,75E-05	290	0,4	18	8,50E-05	213	0,3	Prasojo et al. 2020 *sensu* Parker, 2007	Characteristic flow depth $h_c = (C_f Q_c^2 / g W_{av}^2 S)$^1/3	C_f = bed friction coefficient = 0.002, Q_c = characteristic water discharge = 33385 m3/s, W_{av} = channel width = 669 m, g = gravitational acceleration = 9.8 m/s2, S = slope = 6.75*10E-05 or 8.5*10E-05*
Workflow M7 (grain size)	*Lb = h/S*	17	6,75E-05	256	0,4	14	8,50E-05	163	0,2	Brooke et al. 2020	τ bf50 =(dmS)/(PD50). The resultig mean bankfull chanel depth (15 m) is multiplied with 1.7 to	Dm = mean bankfull channel depth, S = slope = 6.75*10-5 or 8.5*10-5, P = submerged dimensionless density = 1.65 g/cm3, D50 = average grainsize for lowermost portion of the channel = 250 µm, τ bf50= Shields number for dimensionless shear stress = 1.86.

s

Table S6. Obtaining bankfull thalweg channel depth following workflow M4. Bankfull thalweg channel depth is obtained empirically based on bankfull channel width.

mississippi river depth					bankfull height profile from Nittrouer et al. 2011			
river km	river width	depth	absolute depth	moving average	river km	height	river km	height interpolated
0	1301	41	-41	#N/A	0	0	0	0
10	1005	33	-33	#N/A	100	3	10	0,3
20	874	29	-29	#N/A	200	6	20	0,6
30	702	24	-23	#N/A	300	10	30	0,9
40	849	29	-27	-31	400	14	40	1,2
50	750	26	-24	-27	500	18	50	1,5
60	801	27	-25	-26	600	22	60	1,8
70	632	22	-20	-24	700	27	70	2,1
80	867	29	-27	-25	800	33	80	2,4
90	801	27	-24	-24	1000	50	90	2,7
100	674	23	-20	-23			100	3
110	821	28	-24	-23			110	3,3
120	724	25	-21	-23			120	3,6
130	650	23	-19	-22			130	3,9
140	611	22	-17	-20			140	4,2
150	524	19	-14	-19			150	4,5
160	818	28	-23	-19			160	4,8
170	636	22	-17	-18			170	5,1
180	600	21	-16	-18			180	5,4
190	509	18	-13	-17			190	5,7
200	660	23	-17	-17			200	6
210	700	24	-18	-16			210	6,4
220	550	20	-13	-15			220	6,8
230	728	25	-18	-16			230	7,2
240	754	26	-18	-17			240	7,6
250	576	20	-12	-16			250	8
260	534	19	-11	-14			260	8,4
270	658	23	-14	-15			270	8,8
280	1054	34	-25	-16			280	9,2
290	597	21	-12	-15			290	9,6
300	740	25	-15	-15			300	10
310	576	20	-10	-15			310	10,4
320	778	27	-16	-16			320	10,8
330	670	23	-12	-13			330	11,2
340	1041	34	-22	-15			340	11,6
350	718	25	-13	-15			350	12
360	1083	35	-23	-17			360	12,4
370	821	28	-15	-17			370	12,8
380	720	25	-12	-17			380	13,2
390	658	23	-9	-14			390	13,6
400	1103	36	-22	-16			400	14
410	707	24	-10	-14			410	14,4
420	894	30	-15	-14			420	14,8
430	937	31	-16	-14			430	15,2
440	863	29	-13	-15			440	15,6
450	953	32	-16	-14			450	16
460	1060	35	-18	-16			460	16,4
470	742	25	-9	-14			470	16,8
480	836	28	-11	-13			480	17,2
490	1068	35	-17	-14			490	17,6
500	730	25	-7	-12			500	18
510	835	28	-10	-11			510	18,4
520	1070	35	-16	-12			520	18,8
530	1011	33	-14	-13			530	19,2
540	1171	38	-18	-13			540	19,6
550	802	27	-7	-13			550	20
560	911	30	-10	-13			560	20,4
570	690	24	-3	-10			570	20,8
580	1142	37	-16	-11			580	21,2
590	1170	38	-16	-10			590	21,6
600	1356	43	-21	-13			600	22
610	1277	40	-18	-15			610	22,5
620	1150	37	-14	-17			620	23
630	1066	35	-11	-16			630	23,5
640	1270	40	-16	-16			640	24
650	1140	37	-12	-14			650	24,5
660	1098	36	-11	-13			660	25
670	587	21	5	-9			670	25,5
680	1026	34	-8	-8			680	26
690	1554	48	-21	-9			690	26,5
700	997	33	-6	-8			700	27
710	996	33	-5	-7			710	27,6
720	1288	41	-13	-10			720	28,2
730	999	33	-4	-10			730	28,8
740	1273	40	-11	-8			740	29,4
750	1262	40	-10	-9			750	30
760	772	26	4	-7			760	30,6
770	1163	37	-6	-5			770	31,2
780	1314	41	-10	-7			780	31,8
790	1087	35	-3	-5			790	32,4
800	906	30	3	-2			800	33
810	1247	40	-6	-4			810	33,85
820	671	23	11	-1			820	34,7
830	1672	51	-15	-2			830	35,55
840	932	31	5	0			840	36,4
850	618	22	15	2			850	37,25
860	1194	38	0	3			860	38,1
870	1590	49	-10	-1			870	38,95
880	1224	39	1	2			880	39,8
890	873	29	11	4			890	40,65
900	1216	39	3	1			900	41,5
910	1465	46	-3	0			910	42,35
920	954	32	12	5			920	43,2
930	715	25	19	8			930	44,05
940	992	33	12	9			940	44,9
950	551	20	26	13			950	45,75
960	1028	34	13	16			960	46,6
970	717	25	23	19			970	47,45
980	691	24	24	20			980	48,3
990	721	25	24	22			990	49,15
1000	1103	36	14	20			1000	50
1010	1203	38	12	20			1010	50,85
1020	847	29	23	20			1020	51,7
1030	447	16	36	22			1030	52,55
1040	1058	34	19	21			1040	53,4
1050	632	22	32	25			1050	54,25
1060	766	26	29	28			1060	55,1
1070	1000	33	23	28			1070	55,95
1080	743	25	31	27			1080	56,8
1090	614	22	36	30			1090	57,65
1100	551	20	39	32			1100	58,5